

Credit: DESY, Science Communication Lab

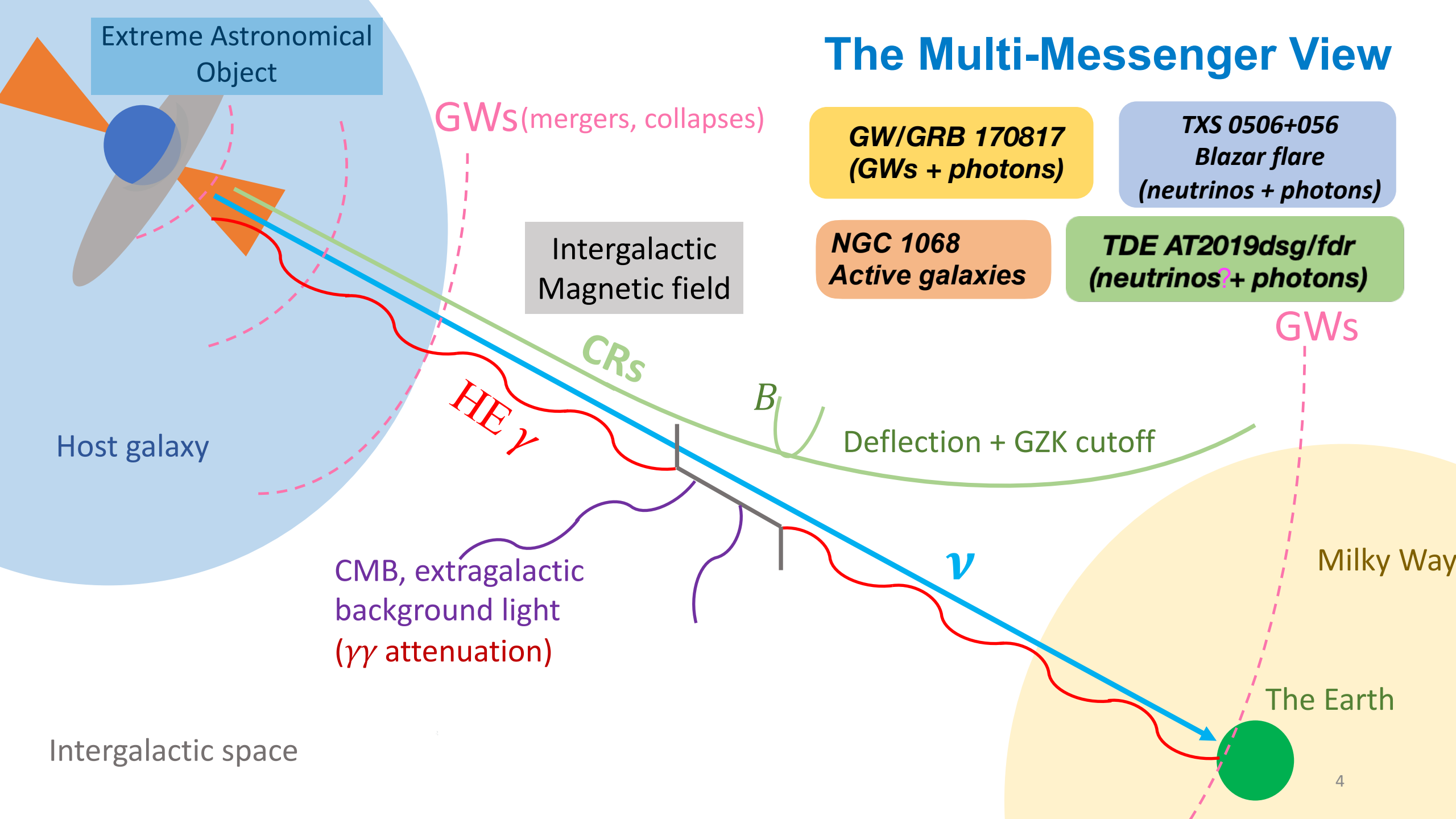
Multi-Messenger Signals of Tidal Disruption Events and Supermassive Black Hole Mergers

Chengchao Yuan
DESY, Zeuthen, Germany

CP3 seminar, UCLouvain
April 26, 2023

HELMHOLTZ





Contents

Electromagnetic cascade and neutrino emission from TDEs

- Observational picture of TDEs
- TDE models
- Neutrinos from TDEs
- EM cascade emission, numerical method
- Implications to neutrino-emitting TDEs, AT2019dsg and AT2019fdr: γ -ray constraints
- Summary and outlook

Jet-induced electromagnetic and neutrino emission from SMBH mergers

- Physical picture and simulations
- Post-merger Jet-cocoon-wind model
- GW-Neutrino detection perspectives
- EM counterparts
- Summary and outlook

Electromagnetic cascade and neutrino emission from TDEs

- Observational picture of TDEs
- TDE models
- Neutrinos from TDEs
- EM cascade emission, numerical method
- Implications to neutrino-emitting TDEs, AT2019dsg and AT2019fdr

Tidal disruption events

When a massive star passes close enough to a SMBH

- The star can be ripped apart by the tidal force at tidal radius (Roche limit)

$$r_T = (2M/m_\star)^{1/3} r_\star \simeq 9 \times 10^{12} \text{ cm} \left(\frac{M}{10^6 M_\odot} \right)^{1/3} \frac{r_\star}{r_\odot} \left(\frac{m_\star}{M_\odot} \right)^{-1/3}$$

- Should be larger than Schwarzschild radius of SMBH,

$$r_s = 2GM/c^2 \simeq 3 \times 10^{11} \text{ cm } M_6$$

- Which yields a theoretical upper limit of SMBH mass in TDE

$$M < 1.6 \times 10^8 M_\odot \left(\frac{r_\star}{r_\odot} \right)^{3/2} \left(\frac{m_\star}{M_\odot} \right)^{-1/2}$$



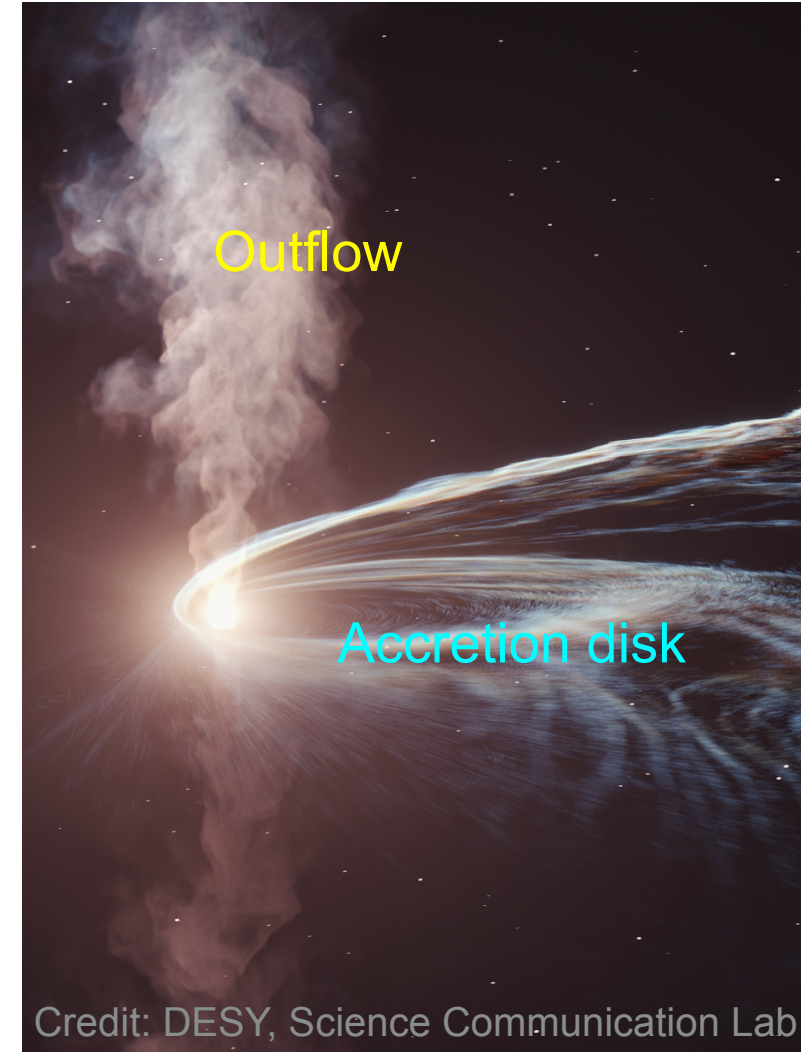
Credit: DESY, Science Communication Lab

Tidal disruption events

When a massive star passes close enough to a SMBH

- ~ half of the star's mass remains bounded by the SMBH gravitational force
- Mass accretion -> months/year-long flare
- Energy to be reprocessed by accretion $\sim 10^{54}$ erg via super-Eddington accretion rate at optical/UV peak

$$\dot{m} = \dot{M}_{\text{peak}} / \dot{M}_{\text{Edd}} \sim 10$$



Credit: DESY, Science Communication Lab

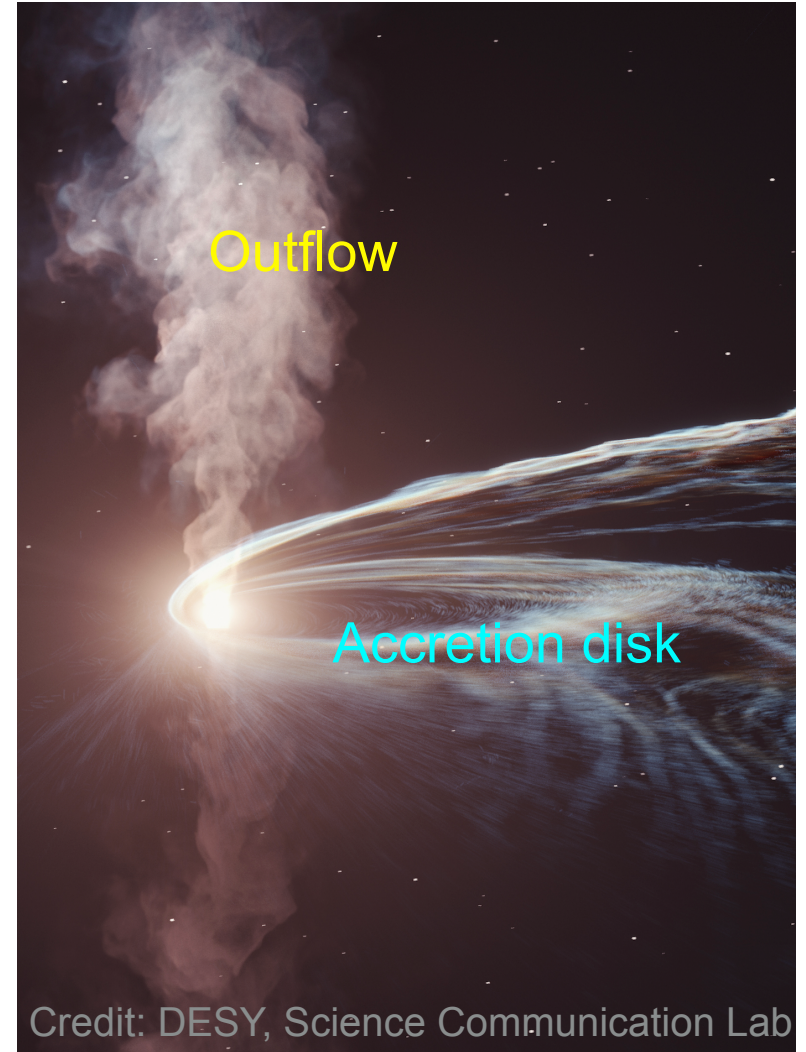
Tidal disruption events

When a massive star passes close enough to a SMBH

- ~ half of the star's mass remains bounded by the SMBH gravitational force
- Mass accretion -> months/year-long flare
- Energy to be reprocessed by accretion $\sim 10^{54}$ erg via super-Eddington accretion rate at optical/UV peak

$$\dot{m} = \dot{M}_{\text{peak}} / \dot{M}_{\text{Edd}} \sim 10$$

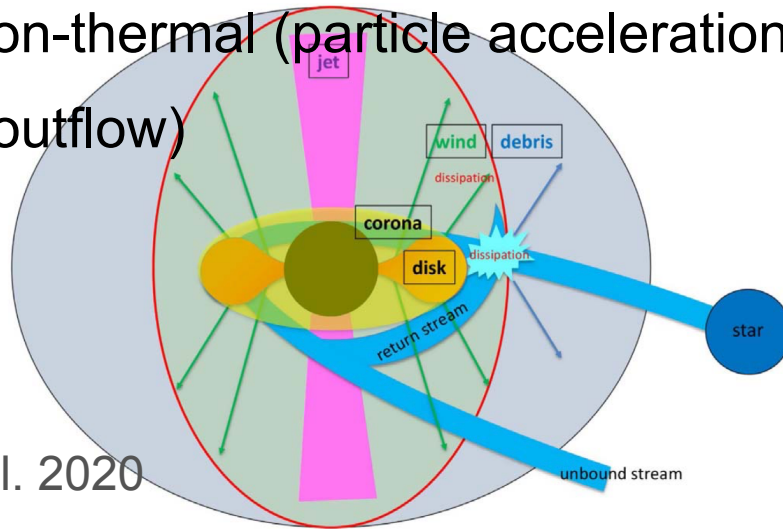
- Multi-wavelength black body (bb) emissions in **optical/UV (O.UV) bands**.
- Some ($\sim 1/4$) TDEs are observed in **X-ray and infrared (IR)** ranges, e.g., AT2019dsg (Stein et al. 2021)



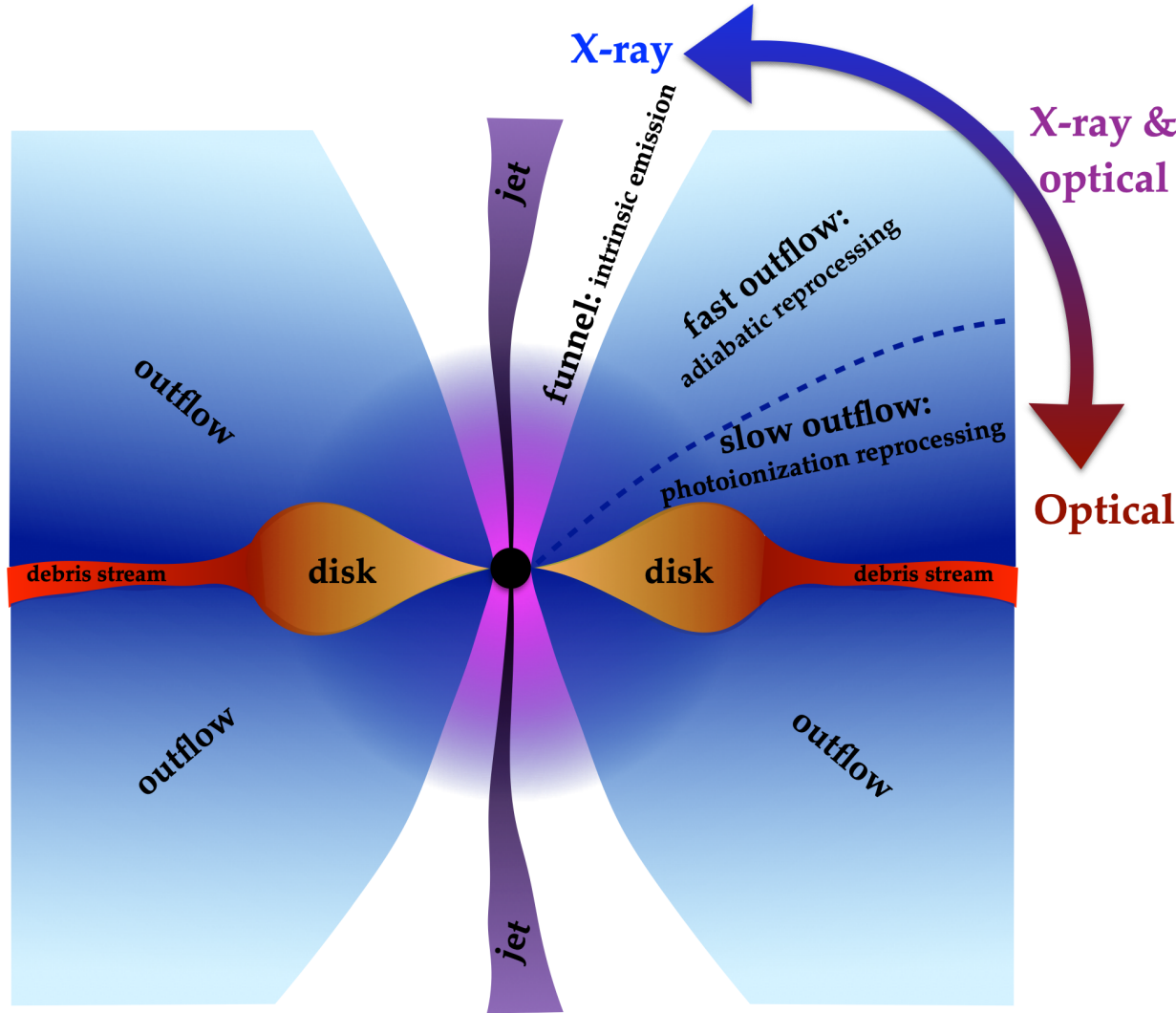
Credit: DESY, Science Communication Lab

TDE models

- **γ -rays:** relativistic jet, EM cascade, wind?
- **X-rays:** close to jet/funnel & hot disk corona
- **Optical/UV:** photosphere (beyond which integrated optical depth < 1)
- **Infrared (IR):** dust-echo
- **Radio:** non-thermal (particle acceleration in disk, jet, outflow)



Murase et al. 2020



Dai et al. 2018

TDE models

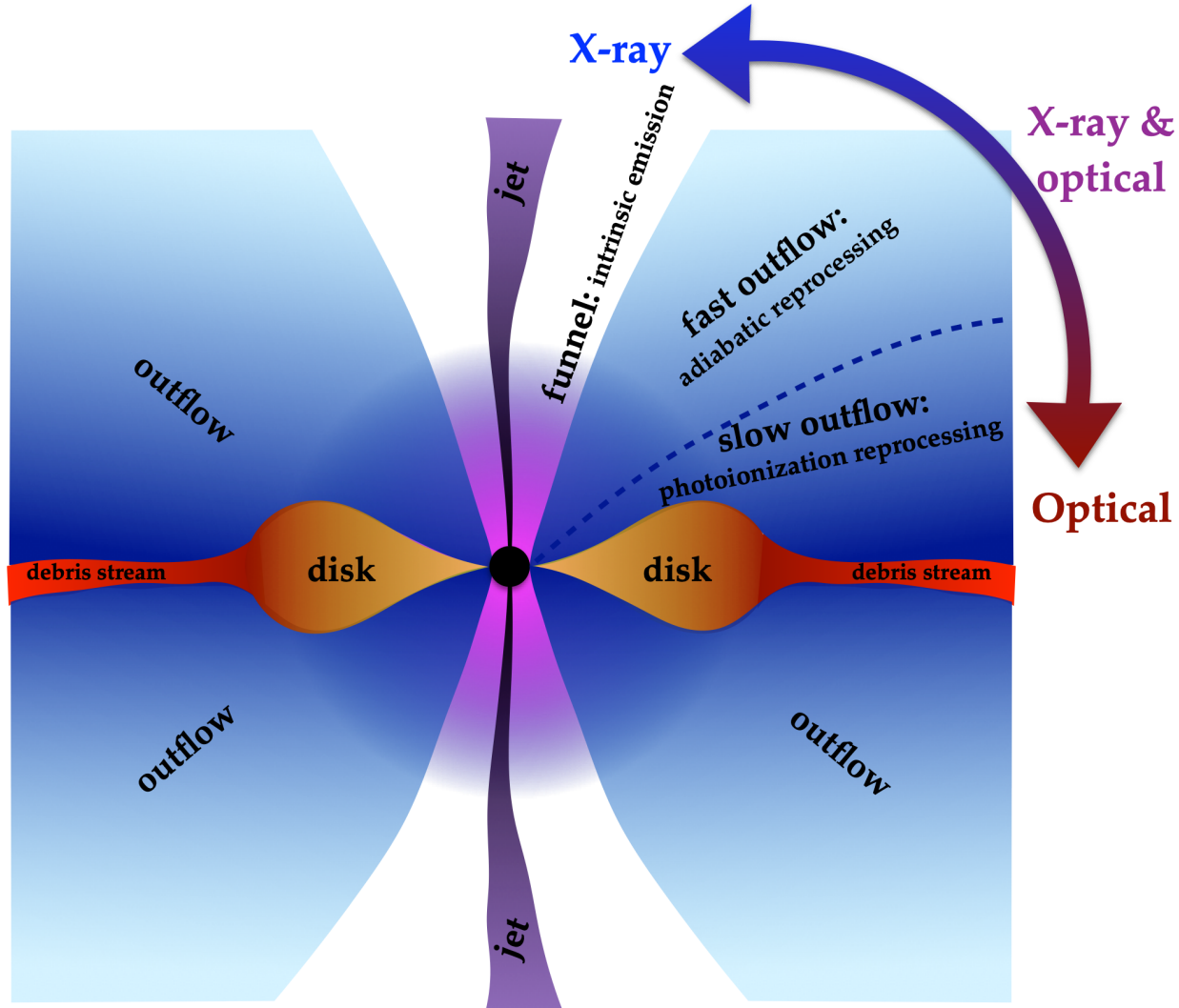
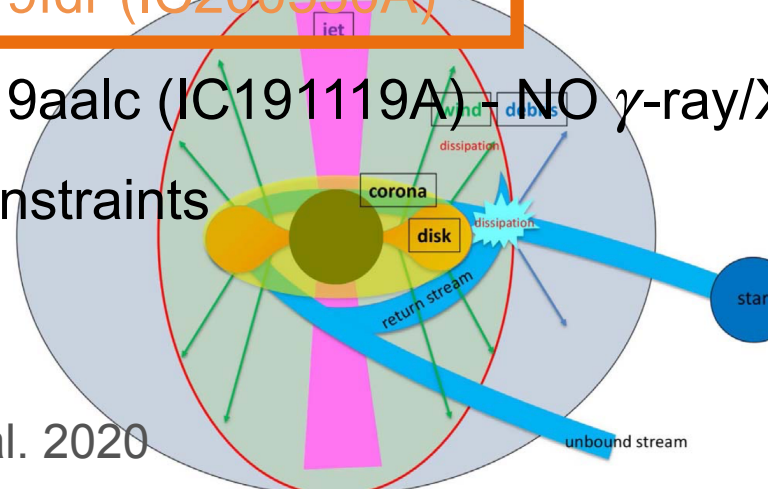
- In addition to the EM signatures, neutrinos might be produced in the **accretion disks, disk winds (outflows), or jets**
- Three TDEs may be associated with IceCube neutrino events

1. [AT2019dsg \(IC191001A\)](#)

2. [AT2019fdr \(IC200530A\)](#)

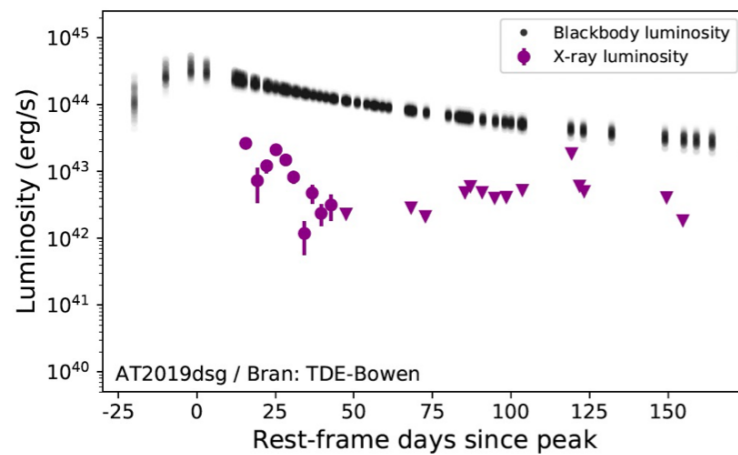
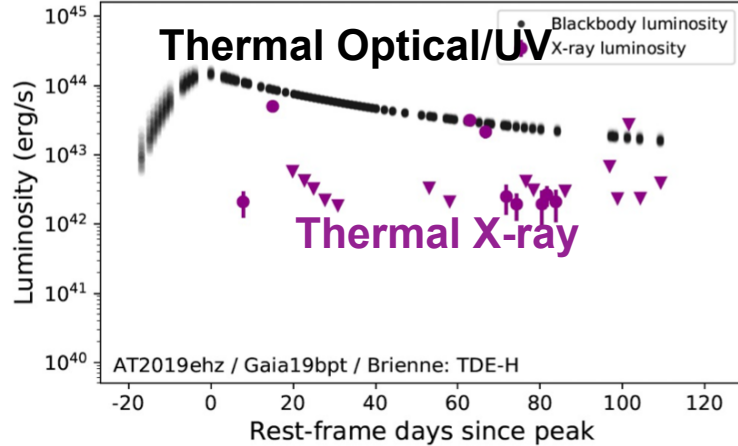
3. AT2019aalc (IC191119A) - NO γ -ray/X-ray constraints

Murase et al. 2020

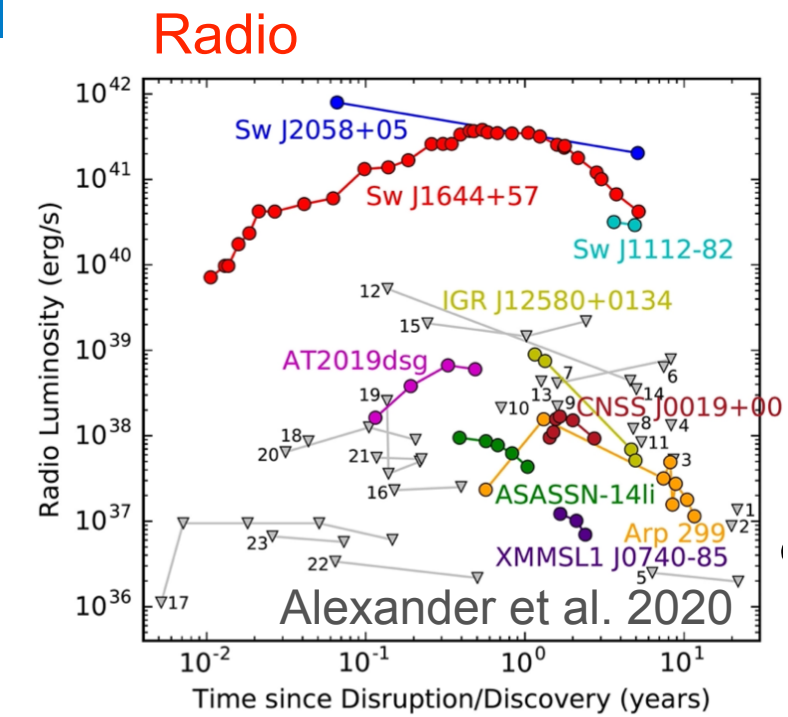
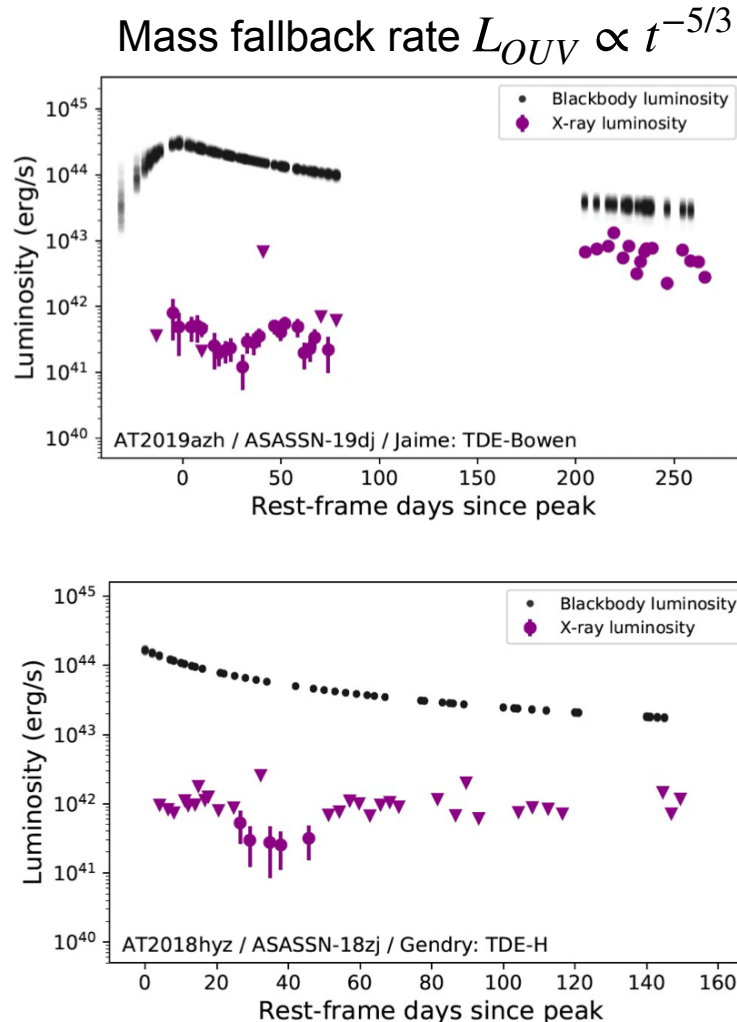


Dai et al. 2018

TDE observational signatures: universal



Van Velzen et al, 2021



A small fraction of TDEs exhibit luminous radio relativistic jet. Most are radio quiet.

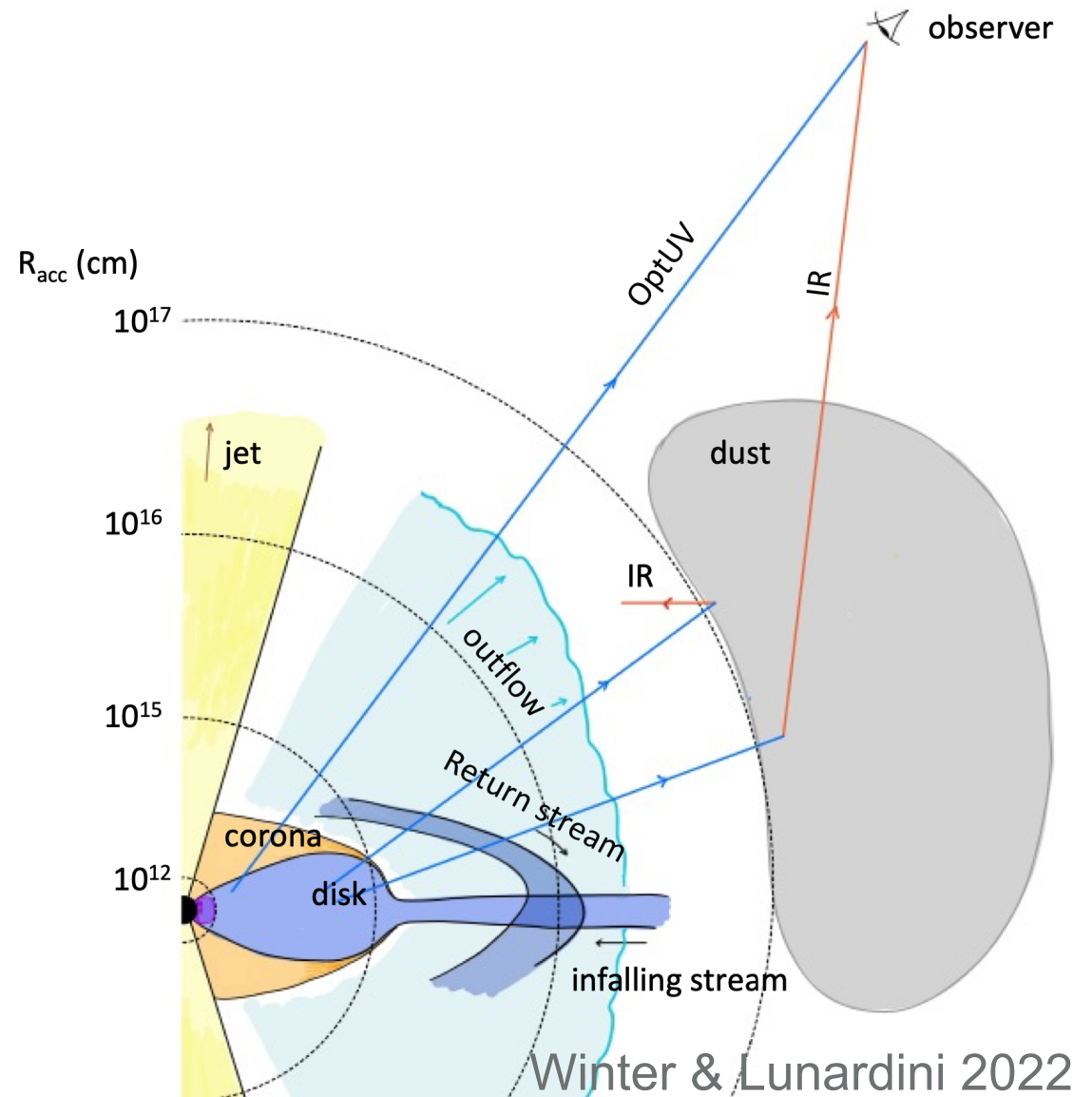
Dust Echo: infrared (IR) emission

X-ray/UV photons heat the dust torus

-> thermal IR emission

- could be detected as the delayed IR emission
- feeds IR photons back to the wind/outflow envelope
- temperature $T_{\text{IR}} \lesssim 0.16 \text{ eV}$ (Reusch et al. 2022)
- IR luminosity can be obtained by convolving $L_{\text{O}UV}$ with a box function $B(T)$, e.g.,
(Reusch et al. 2022, Winter & Lunardini 2022)

$$L_{\text{IR}}(t) \propto \int L_{\text{O}UV}(t')B(t - t')dt'$$

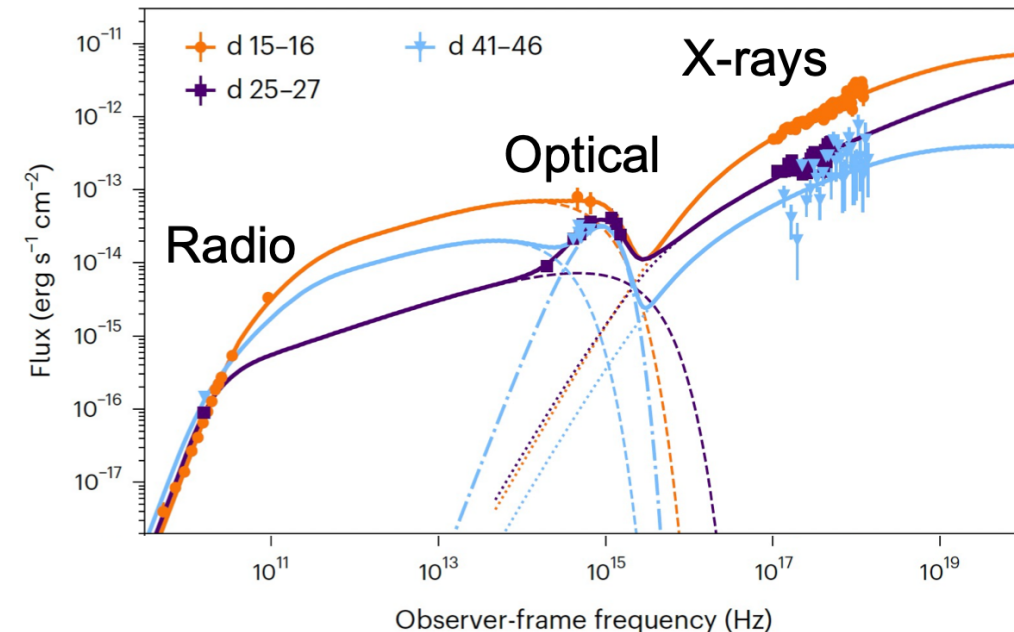
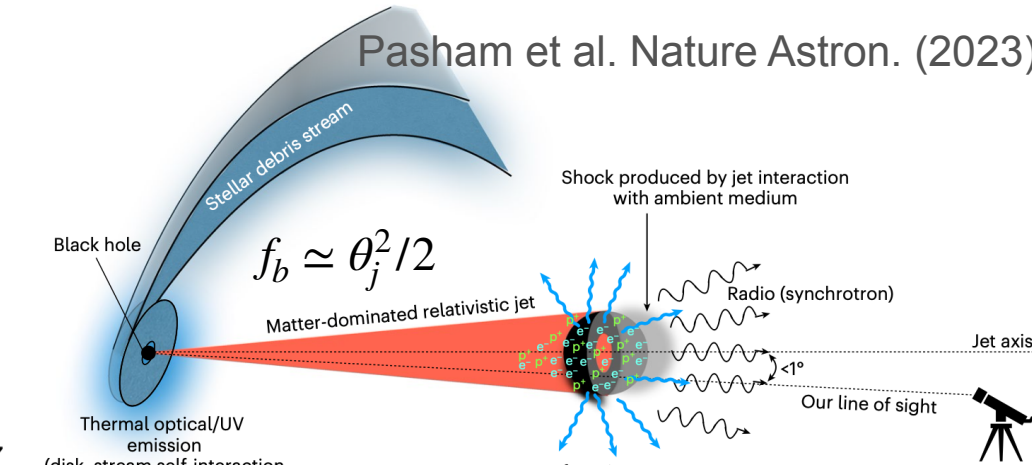
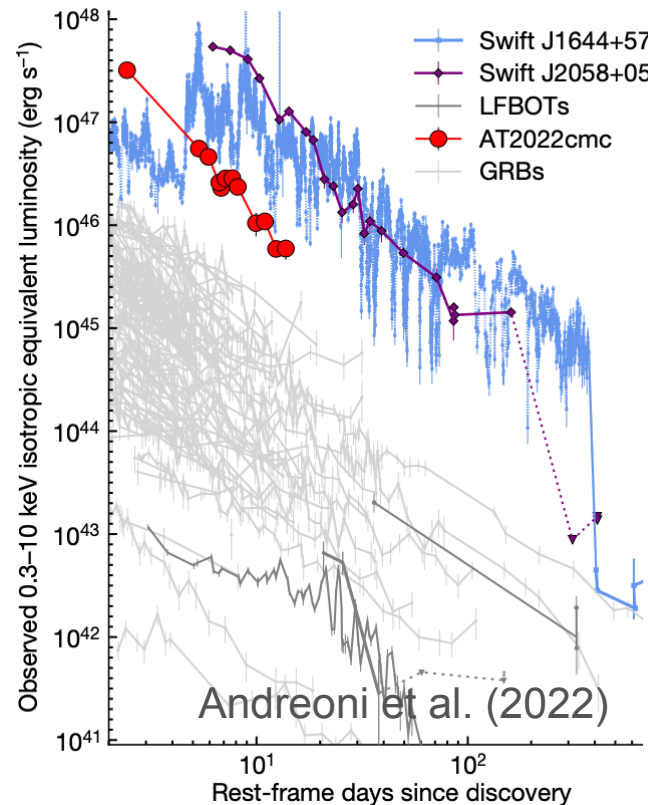


Jetted TDEs

A recent example: AT2022cmc

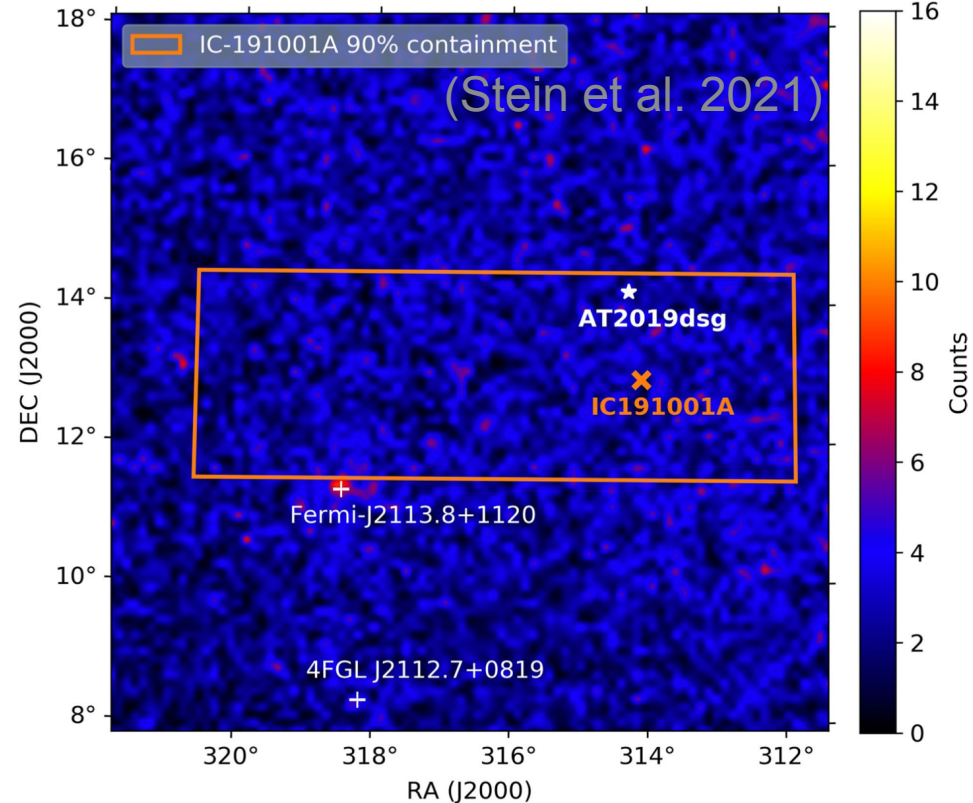
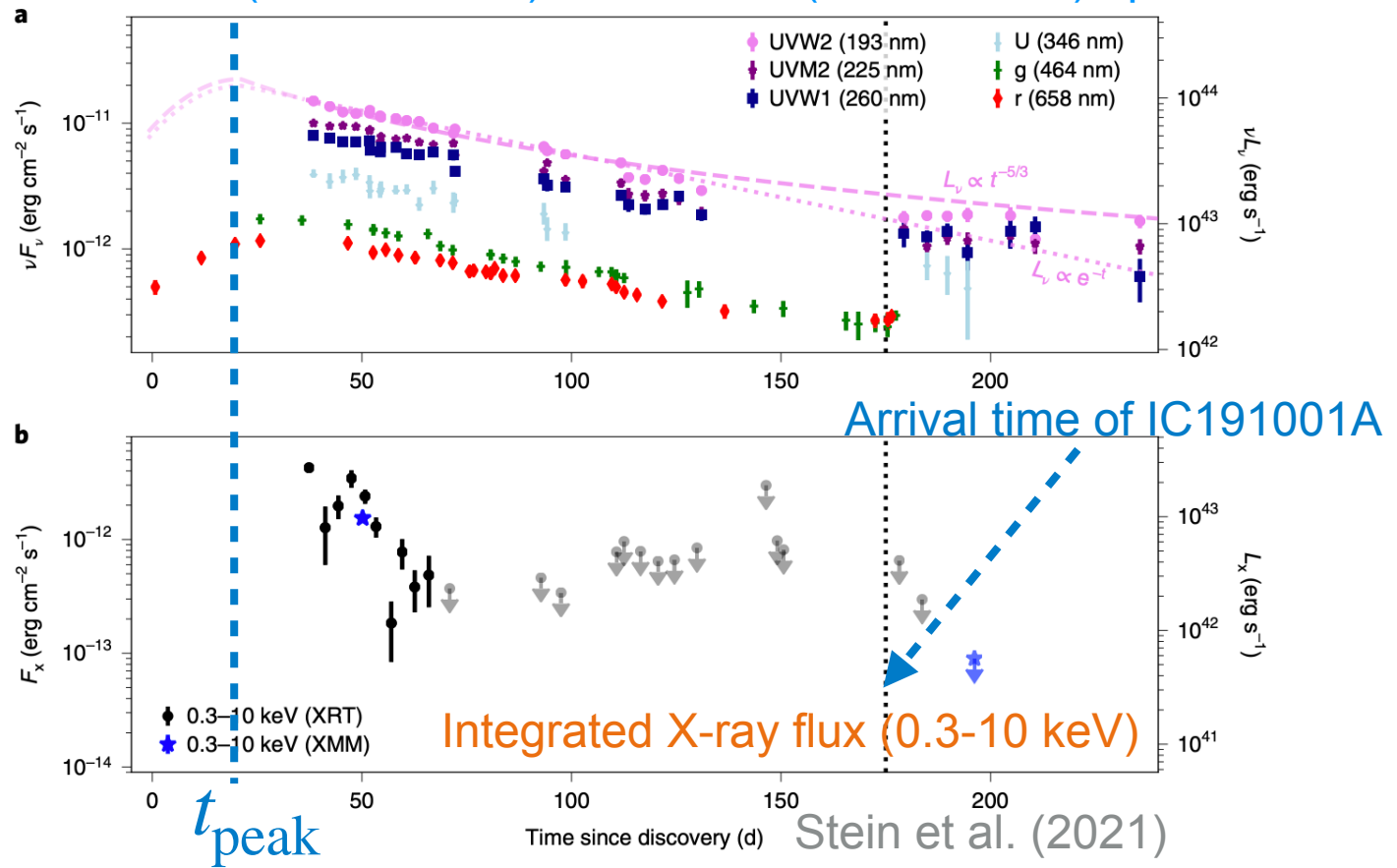
(In addition to Swift J1644+57 and Swift J2058+05)

- $z = 1.193$
- Very bright
- Non-thermal X-rays may be produced by relativistic jets ($\gtrsim 10^{48}$ erg/s, usually 10^{42-44} erg/s)
- A very high Lorentz factor $\Gamma \sim 90$ is assumed (~ 10 for blazars)



AT2019dsg: no jet or off-axis

- ZTF (optical: g, r) + Swift UVOT (UV)
- Swift-XRT/XMM-Newton: X-ray (0.3-10 keV)
- $z \sim 0.051$
- *Fermi* (0.1-800 GeV) and HAWC (0.3-100 TeV) up limits

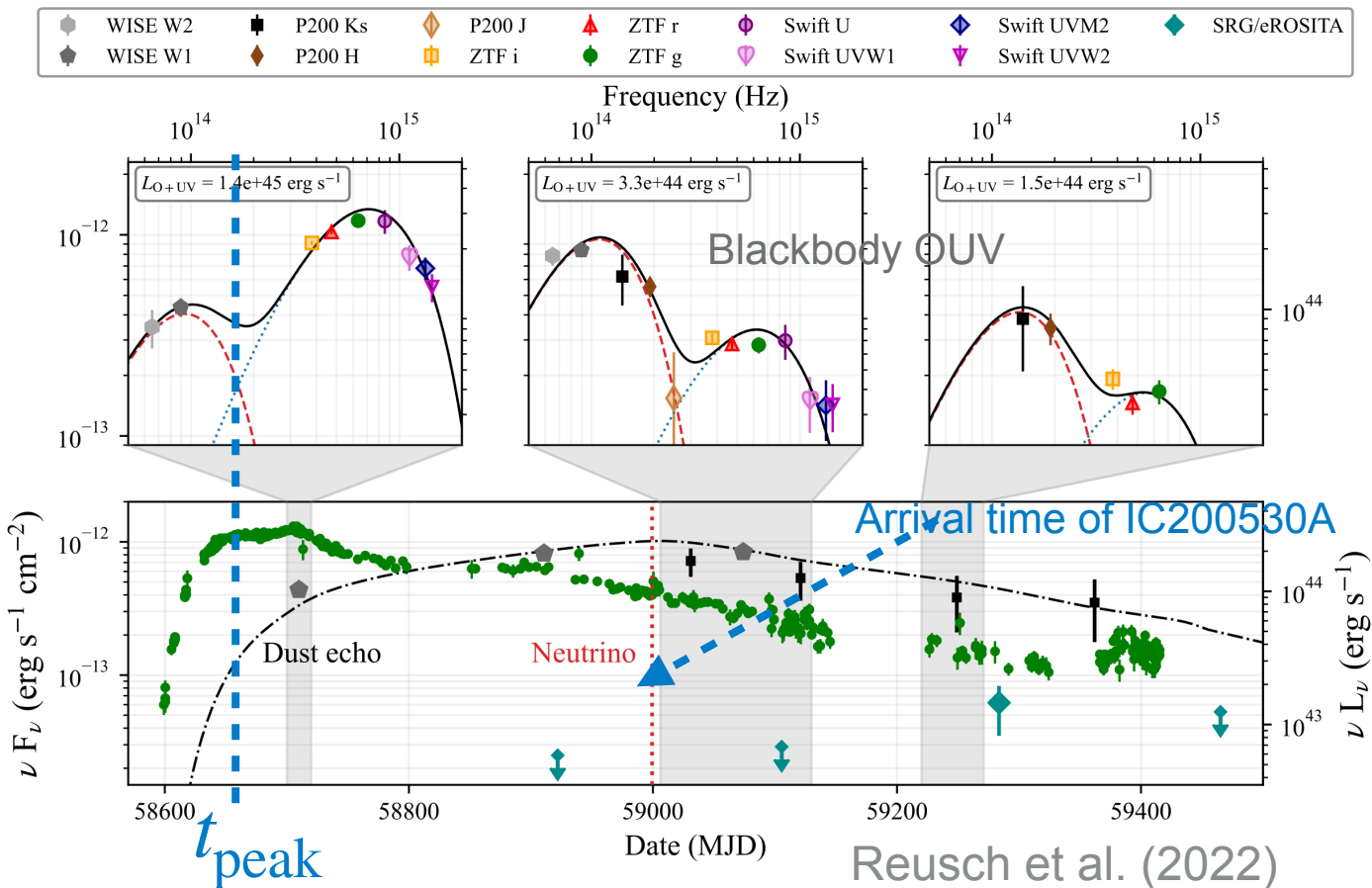


Measured black body spectra:

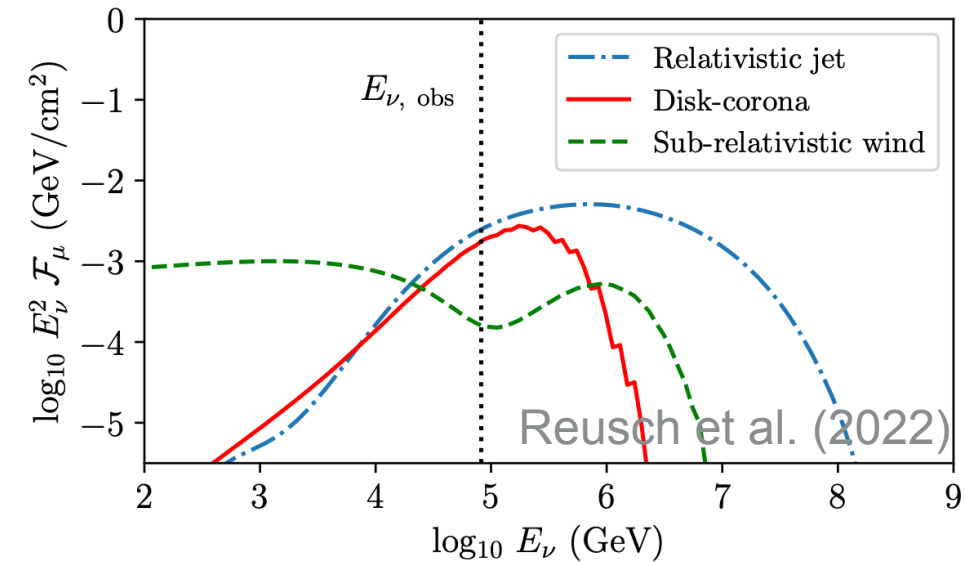
- **X-ray:** $T_X = 72$ eV, from hot accretion disk
- **OUV:** $T_{\text{OUV}} = 3.4$ eV, from photosphere (nearly constant)
- **IR:** $T_{\text{IR}} = 0.15$ eV (dust echo)

AT2019fdr: no jet or off-axis

- ZTF (optical: g, r) + Swift UVOT (UV) + IR
- Swift-XRT: X-ray (0.3-10 keV)
- $z \sim 0.267$
- *Fermi* up limit ✓



AT2019fdr lies in 90% localization of IC200530A: three site scenario

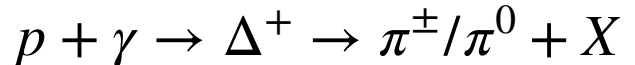


Measured black body spectra:

- **X-ray:** $T_X = 56 \text{ eV}$, from hot accretion disk
- **UV:** $T_{\text{UV}} = 1.2 \text{ eV}$, from photosphere (nearly constant)
- **IR:** $T_{\text{IR}} = 0.15 \text{ eV}$ (dust echo)

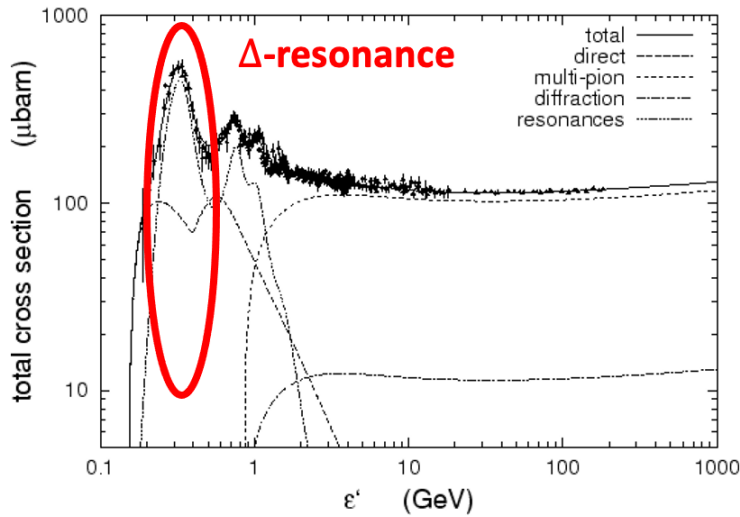
Production of High-Energy Astrophysical Neutrinos

Photo-pion/meson ($p\gamma$) process

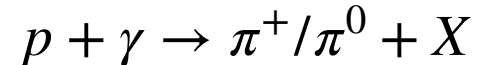


Ingredients: dense (low-energy) photons [IR/OUV/X-ray photons in TDE] + CRs in luminous objects

Delta resonance proton energy: $E_p \gtrsim \frac{m_\pi(2m_p + m_\pi)c^2}{4\varepsilon_\gamma}$



Hadronuclear (pp) process



Ingredients: dense thermal/rest target protons [outflows/winds in TDEs] + CRs

In TDE model, depends on the wind params, subdominant even in optimistic case

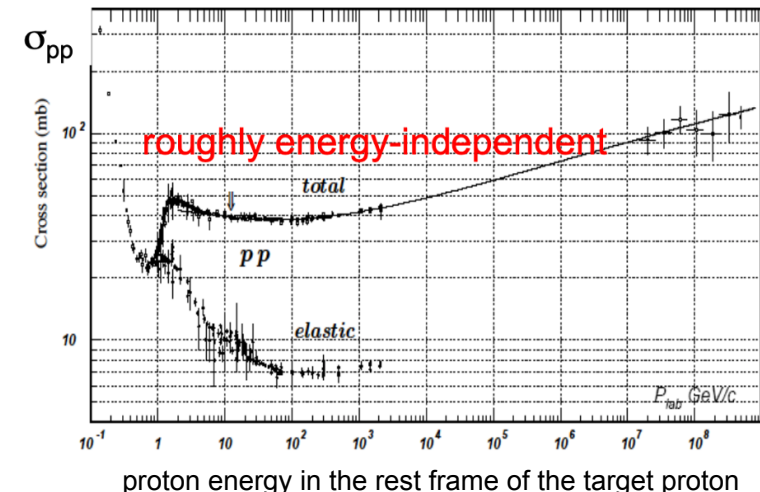
$$\begin{aligned} \pi^\pm &\rightarrow \mu^\pm + \nu_\mu(\bar{\nu}_\mu), \quad \mu^\pm \rightarrow e^\pm + \bar{\nu}_\mu(\nu_\mu) + \nu_e(\bar{\nu}_e) \\ \pi^0 &\rightarrow \gamma + \gamma \end{aligned}$$

$$\varepsilon_\nu Q_{\varepsilon_\nu} \approx \frac{3K}{4(K+1)} e^{-f_{pp,p\gamma}} (\varepsilon_p Q_{\varepsilon_p})|_{\varepsilon_p \sim 20\varepsilon_\nu}$$

$$\varepsilon_\gamma Q_{\varepsilon_\gamma} \approx \frac{4}{3K} \varepsilon_\nu Q_{\varepsilon_\nu}|_{\varepsilon_\gamma \sim 2\varepsilon_\nu}$$

$$pp : K = N_{\pi^\pm}/N_{\pi^0} \sim 2$$

$$p\gamma : K = N_{\pi^\pm}/N_{\pi^0} \sim 1$$



Radiation processes

Neutrino production: $p\gamma/p\bar{p} \rightarrow \pi^\pm \rightarrow \nu_e \bar{\nu}_e \nu_\mu \bar{\nu}_\mu$

synchrotron/SSC: $(e^\pm) \xrightarrow[\text{magnetic field}]{} (e^\pm)' + \gamma, (e^\pm)' + \gamma \rightarrow (e^\pm)'' + \gamma'$

Proton synchrotron: $p \xrightarrow[\text{magnetic field}]{} \gamma + p'$

Cascade processes: $\pi^0 \rightarrow 2\gamma$

$p\gamma_{\text{bb}}/p\bar{p} \rightarrow \pi^\pm \rightarrow (\mu^\pm)(e^\pm) \xrightarrow[\text{magnetic field}]{} (\mu^\pm)'(e^\pm)' + \gamma, (e^\pm)' + \gamma \rightarrow (e^\pm)'' + \gamma'$

$\gamma\gamma \rightarrow (e^\pm) \xrightarrow[\text{magnetic field}]{} (e^\pm)' + \gamma, (e^\pm)' + \gamma \rightarrow (e^\pm)'' + \gamma'$

Bethe-Heitler (BH) pair production $p\gamma_{\text{bb}} \rightarrow p'(e^\pm) \xrightarrow[\text{magnetic field}]{} (e^\pm)' + \gamma, (e^\pm)' + \gamma \rightarrow (e^\pm)'' + \gamma'$

Particle cooling:

$p \rightarrow p'$

$(e^\pm) \rightarrow (e^\pm)' \rightarrow (e^\pm)''$

$(\mu^\pm) \rightarrow (\mu^\pm)'$

Electromagnetic cascade and neutrino emission from TDEs

- Numerical methods, EM cascade emission from AT2019dsg/AT2019fdr
- Implications to neutrino-emitting TDEs, AT2019dsg and AT2019fdr: γ -ray constraints

AM3: Astrophysical Multiwavelength and MultiMessenger

An open-source tool for lepton-hadronic modeling of astrophysical sources

Numerically solving the coupled PDEs for electron, proton, neutrino and photon distributions. (Gao et al. 2017)

$$\partial_t n(\gamma, t) = -\partial_\gamma \{ \dot{\gamma}(\gamma, t) n(\gamma, t) - \partial_\gamma [D(\gamma, t) n(\gamma, t)]/2 \} - \alpha(\gamma, t) n(\gamma, t) + Q(\gamma, t)$$

Cooling Diffusion Escape/Advection Injection

Electrons/positrons

$$\partial_t N_e = -\partial_x [A_e \cdot N_e - B_e \cdot \partial_x N_e] - (\alpha_{e,esc} + \alpha_{e,annih}) N_e + \epsilon_{e,ext} + \sum \epsilon_{e,internal}$$

Neutrinos

$$\partial_t N_\nu = -\alpha_{\nu,esc} N_\nu + \sum \epsilon_{\nu,int}$$

Photons

$$\partial_t N_\gamma = -(\alpha_{\gamma,esc} + \alpha_{\gamma,ssc} + \alpha_{\gamma,ic} + \alpha_{\gamma,\gamma\gamma} + \alpha_{\gamma,BH} + \alpha_{\gamma,pp}) N_\gamma + \epsilon_{\gamma,ext} + \sum \epsilon_{\gamma,internal}$$

Protons

$$\partial_t N_p = -\partial_x [A_p \cdot N_p - B_p \cdot \partial_x N_p] - (\alpha_{p,esc} + \alpha_{p,pp} + \alpha_{p,py}) N_p + \epsilon_{p,ext}$$

Intermediate particles: μ^\pm, π^\pm, π^0

For electrons,

$$N_e(x, t) = \frac{dN_e}{dVd \ln \gamma_e}, x = \ln \gamma_e$$

Escape terms: $\alpha_{e,i}(x)$

Cooling & diffusion terms:

$$A_e = \dot{\gamma}_e/\gamma_e - \partial_{\gamma_e} [D_e(\gamma_e)/\gamma_e]/2$$

$$B_e = D_e(\gamma_e)/(2\gamma_e)$$

Injection terms:

$$\epsilon_{e,i} = \gamma_e Q_{e,i}$$

AM3: Astrophysical Multiwavelength and MultiMessenger

An open-source tool for lepton-hadronic modeling of astrophysical sources

Numerically solving the coupled PDEs for electron, proton, neutrino and photon distributions. (Gao et al. 2017)

$$\partial_t n(\gamma, t) = -\partial_\gamma \{ \dot{\gamma}(\gamma, t) n(\gamma, t) - \partial_\gamma [D(\gamma, t) n(\gamma, t)]/2 \} - \alpha(\gamma, t) n(\gamma, t) + Q(\gamma, t)$$

Cooling **Diffusion** **Escape/Advection** **Injection**

Electrons/positrons

$$\partial_t N_e = -\partial_x [A_e \cdot N_e - B_e \cdot \partial_x N_e] - (\alpha_{e,esc} + \alpha_{e,annih}) N_e + \epsilon_{e,ext} + \sum \epsilon_{e,internal}$$

Neutrinos

$$\partial_t N_\nu = -\alpha_{\nu,esc} N_\nu + \sum \epsilon_{\nu,int}$$

Photons

$$\partial_t N_\gamma = -(\alpha_{\gamma,esc} + \alpha_{\gamma,ssc} + \alpha_{\gamma,ic} + \alpha_{\gamma,\gamma\gamma} + \alpha_{\gamma,BH} + \alpha_{\gamma,pp}) N_\gamma + \epsilon_{\gamma,ext} + \sum \epsilon_{\gamma,internal}$$

Protons

$$\partial_t N_p = -\partial_x [A_p \cdot N_p - B_p \cdot \partial_x N_p] - (\alpha_{p,esc} + \alpha_{p,pp} + \alpha_{p,py}) N_p + \epsilon_{p,ext}$$

Developers:

- Shan Gao (DESY),
- Xavier Rodrigues (RUB, DESY),
- Annika Rudolph (NBI, DESY),
- Marc Klinger (DESY),
- Chengchao Yuan (DESY),
- Gaetan Clairfontaine (U. Würzburg)

Code publication in preparation!

AM3: Astrophysical Multiwavelength and MultiMessenger

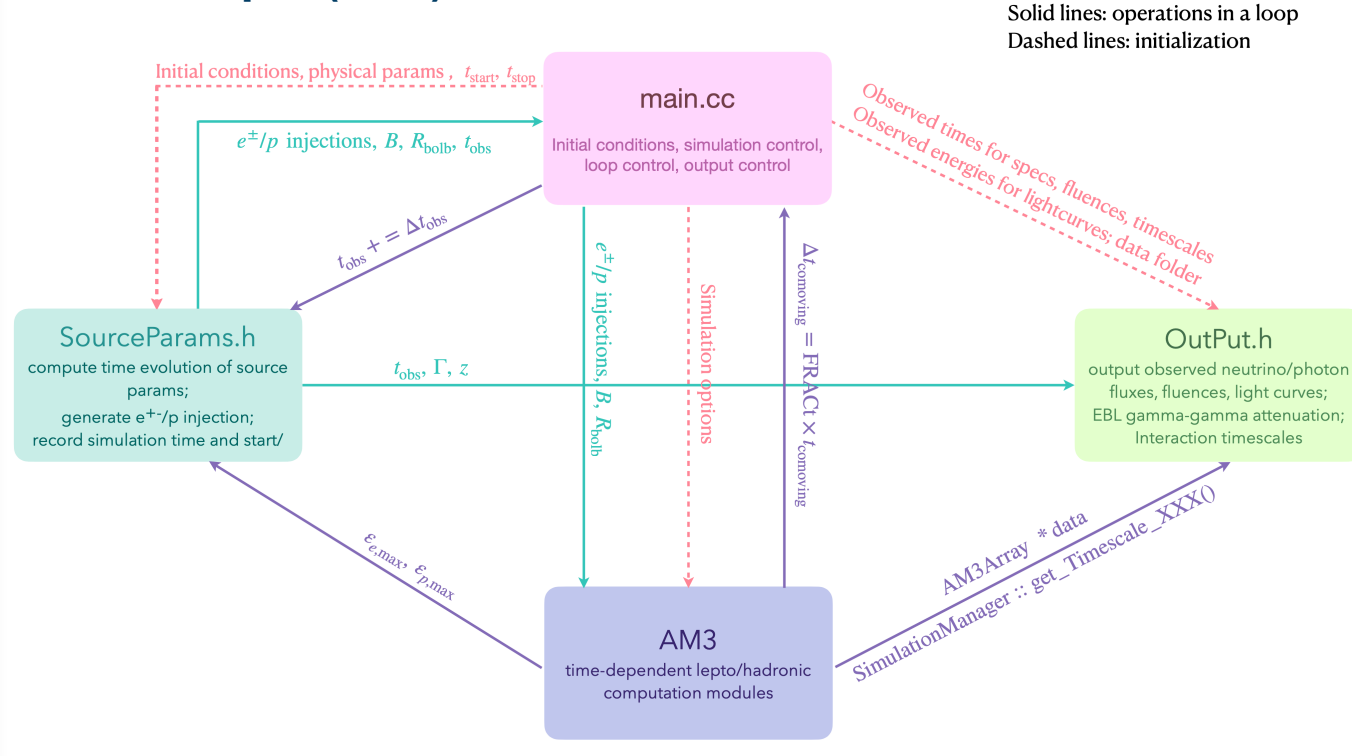
An open-source tool for lepton-hadronic modeling of astrophysical sources

Numerically solving the coupled PDEs for electron, proton, neutrino and photon distributions. (Gao et al. 2017)

$$\partial_t n(\gamma, t) = -\partial_\gamma \{ \dot{\gamma}(\gamma, t)n(\gamma, t) - \partial_\gamma [D(\gamma, t)n(\gamma, t)]/2 \} - \alpha(\gamma, t)n(\gamma, t) + Q(\gamma, t)$$

Cooling **Diffusion** **Escape/Advection** **Injection**

One example (C++)



To turn on/off each process:

```
sim.process_ac = 1;
sim.process_in = 2;
sim.process_ic = 1;
sim.process_sy = 1;
sim.process_pp = 1;
sim.process_bh = 1;
sim.process_pg = 1;
sim.process_es = 1;
sim.process_psy = 1;
sim.process_pic = 1 ;
sim.process_sy_mu = 1;
sim.process_ic_mu = 1;
sim.process_sy_pi = 1;
sim.process_ic_pi = 1;
```

AM3: Astrophysical Multiwavelength and MultiMessenger

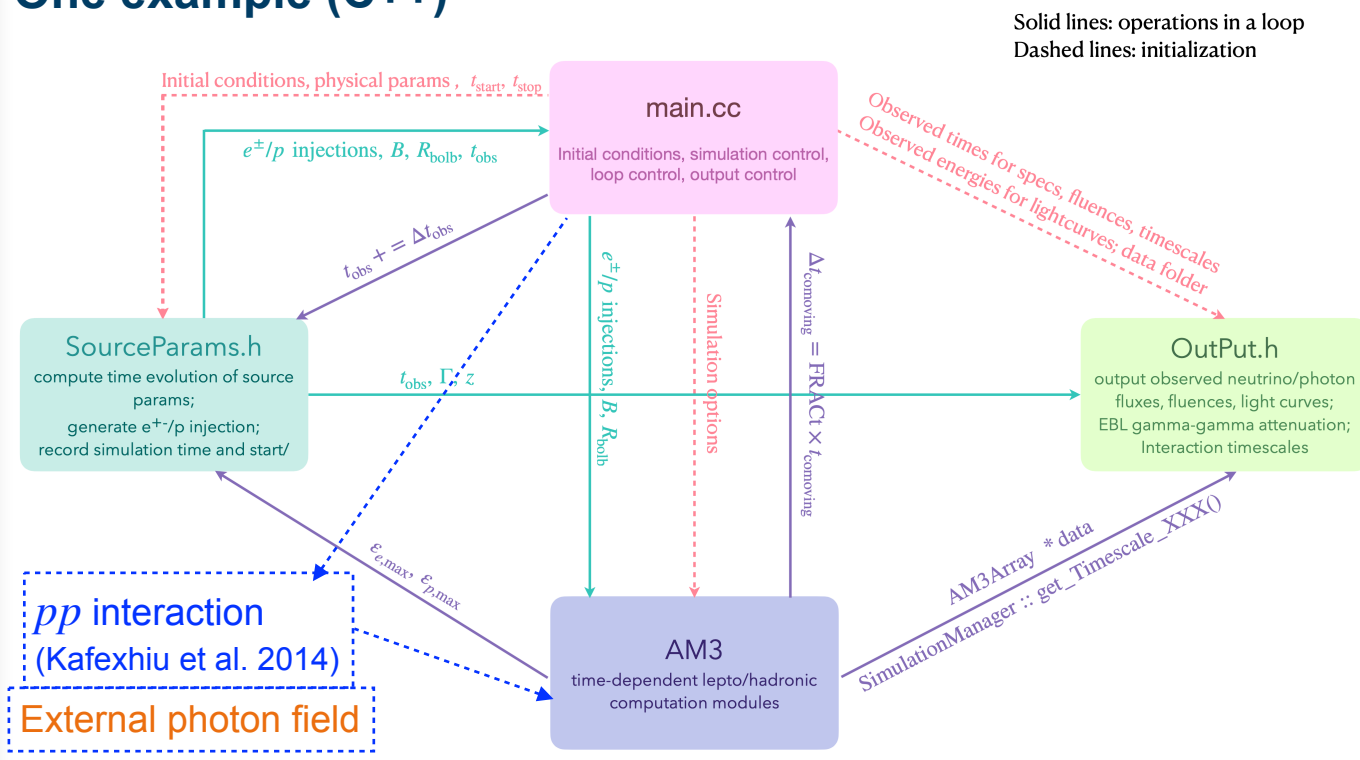
An open-source tool for lepton-hadronic modeling of astrophysical sources

Numerically solving the coupled PDEs for electron, proton, neutrino and photon distributions. (Gao et al. 2017)

$$\partial_t n(\gamma, t) = -\partial_\gamma \{ \dot{\gamma}(\gamma, t)n(\gamma, t) - \partial_\gamma [D(\gamma, t)n(\gamma, t)]/2 \} - \alpha(\gamma, t)n(\gamma, t) + Q(\gamma, t)$$

Cooling **Diffusion** **Escape/Advection** **Injection**

One example (C++)



To turn on/off each process:

```
sim.process_ac = 1;  
sim.process_in = 2;  
sim.process_ic = 1;  
sim.process_sy = 1;  
sim.process_pp = 1;  
sim.process_bh = 1;  
sim.process_pg = 1;  
sim.process_es = 1;  
sim.process_psy = 1;  
sim.process_pic = 1 ;  
sim.process_sy_mu = 1;  
sim.process_ic_mu = 1;  
sim.process_sy_pi = 1;  
sim.process_ic_pi = 1;
```

AM3: Astrophysical Multiwavelength and MultiMessenger

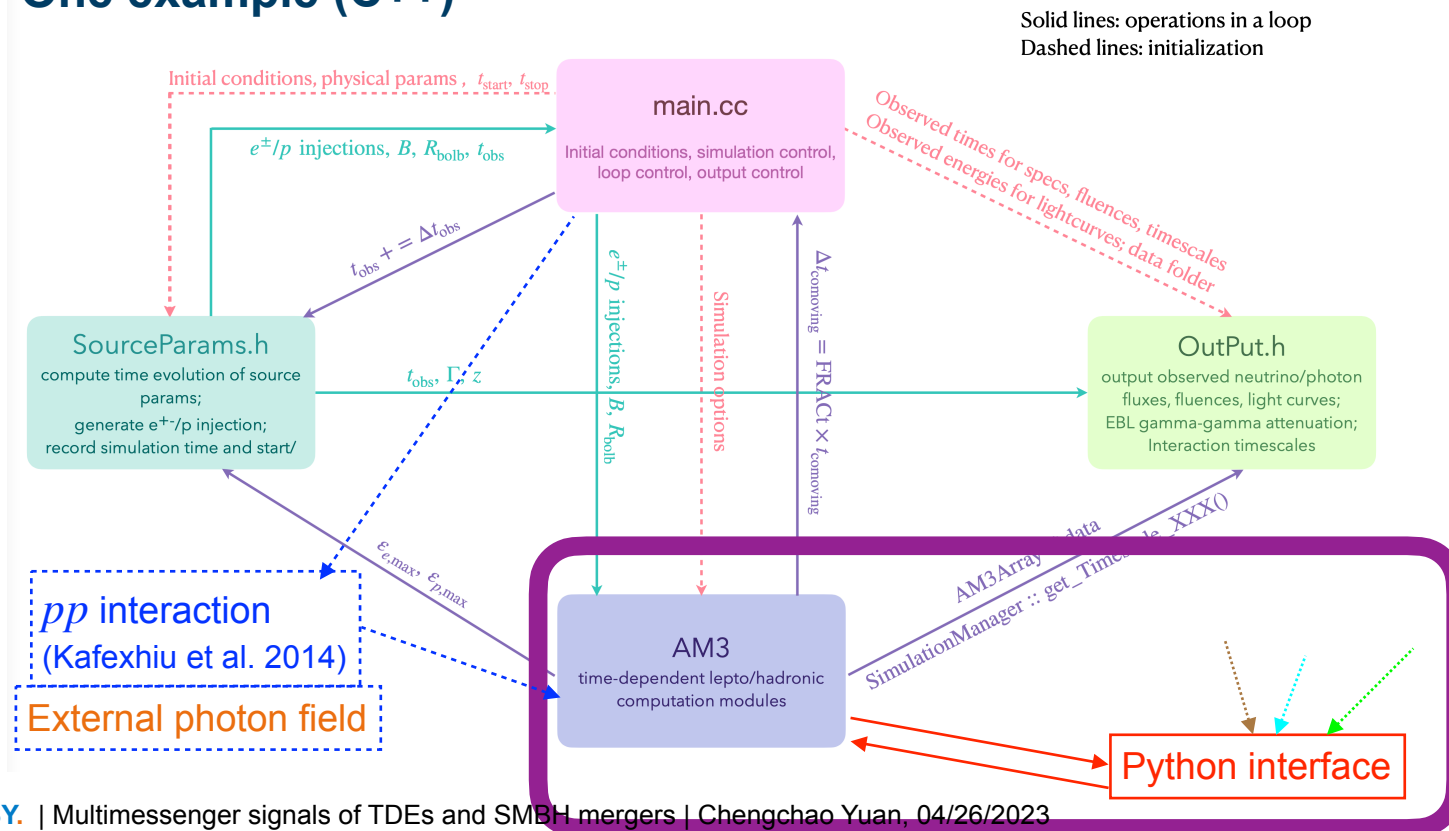
An open-source tool for lepton-hadronic modeling of astrophysical sources

Numerically solving the coupled PDEs for electron, proton, neutrino and photon distributions. (Gao et al. 2017)

$$\partial_t n(\gamma, t) = -\partial_\gamma \{ \dot{\gamma}(\gamma, t)n(\gamma, t) - \partial_\gamma [D(\gamma, t)n(\gamma, t)]/2 \} - \alpha(\gamma, t)n(\gamma, t) + Q(\gamma, t)$$

Cooling **Diffusion** **Escape/Advection** **Injection**

One example (C++)



To turn on/off each process:

```
sim.process_ac = 1;
sim.process_in = 2;
sim.process_ic = 1;
sim.process_sy = 1;
sim.process_pp = 1;
sim.process_bh = 1;
sim.process_pg = 1;
sim.process_es = 1;
sim.process_psy = 1;
sim.process_pic = 1 ;
sim.process_sy_mu = 1;
sim.process_ic_mu = 1;
sim.process_sy_pi = 1;
sim.process_ic_pi = 1;
```

Proton injection

Four parameters: $E_{p,\min} \sim 1$ GeV, spectra index $p = 2$, $E_{p,\max}$ (free-param), normalization factor

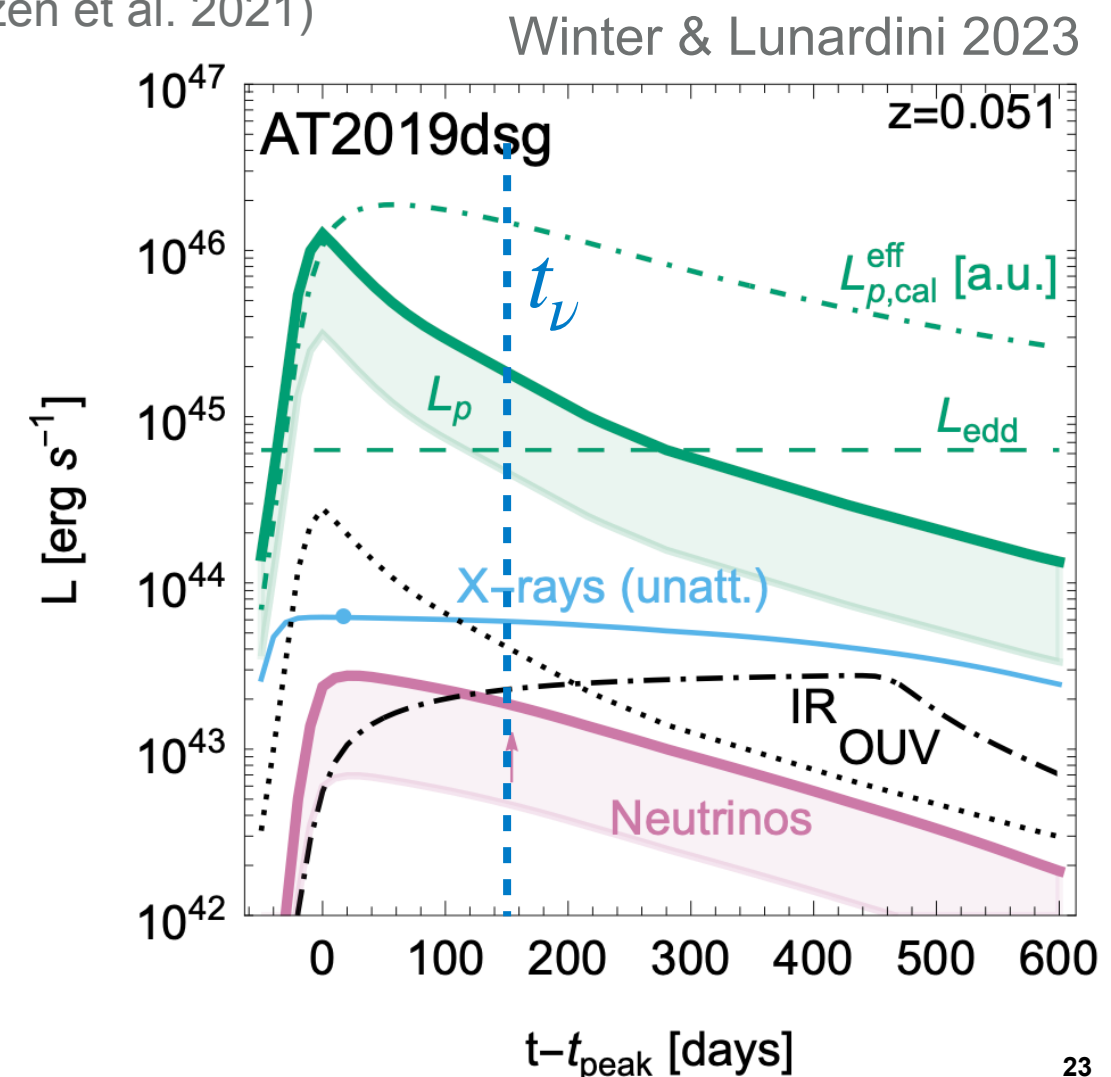
Example - AT2019dsg: $M_{\text{SMBH}} \simeq 5 \times 10^6 M_\odot$ (van Velzen et al. 2021)

We use four parameters to determine the proton injection (**do not specify the accelerator**)

- Normalization $\int dE_p E_p \dot{Q}(E_p) = L_p / (4\pi R^3 / 3)$
- $L_p(t) = \epsilon_{\text{diss}} \dot{M}_*(t) c^2$

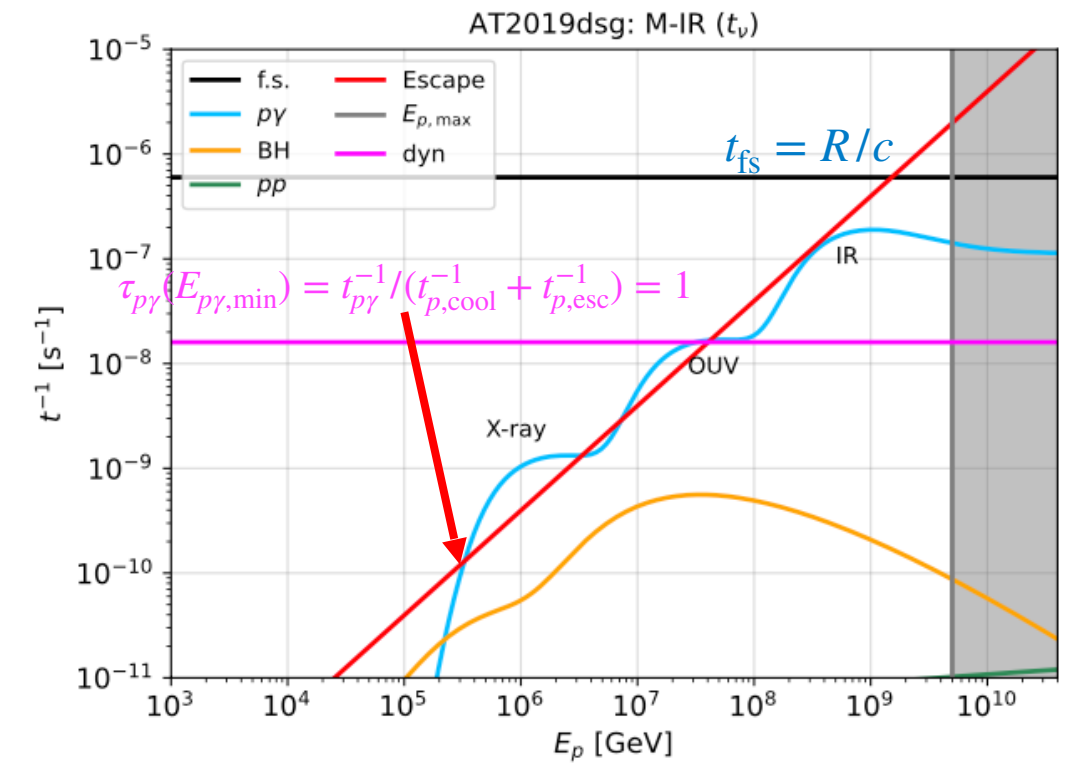
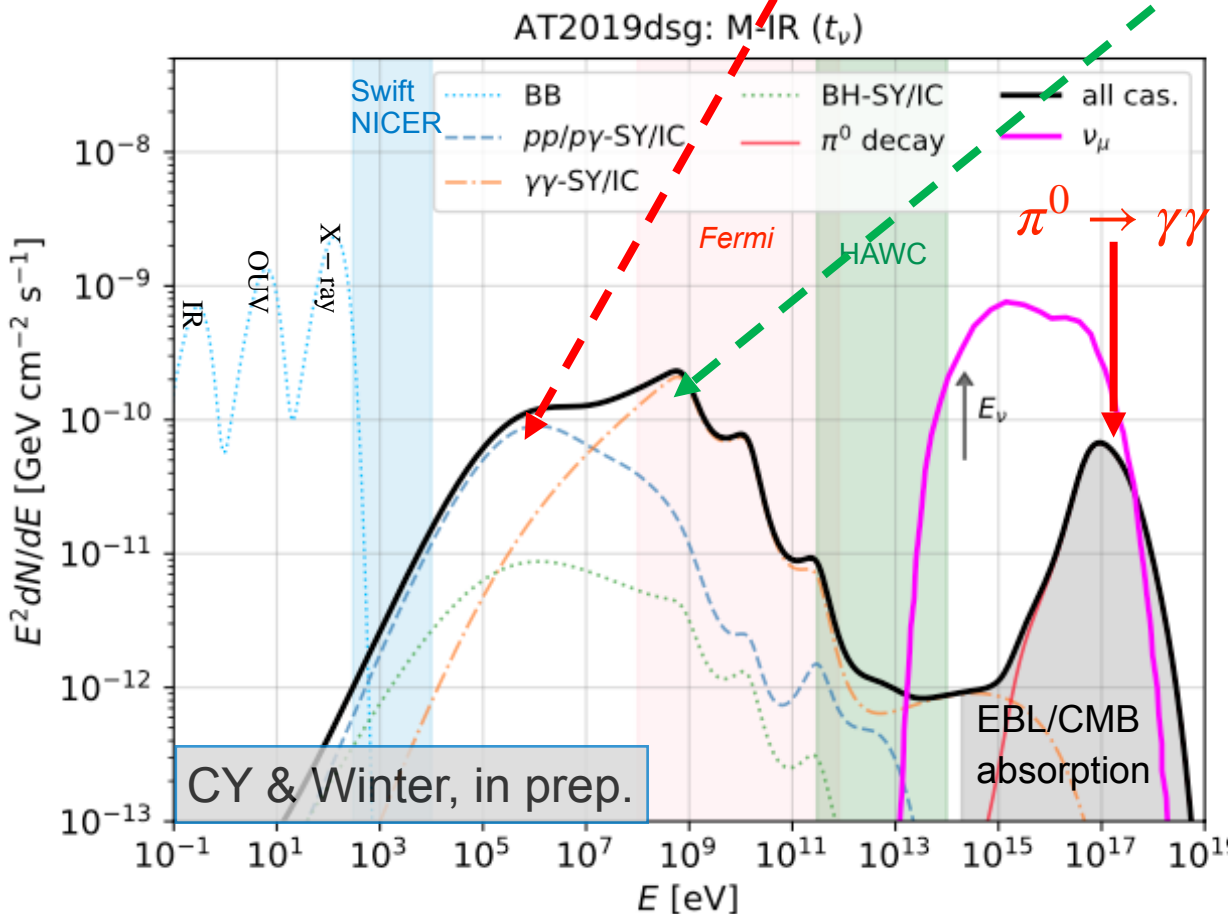
Assumptions

- $\dot{M}_*(t)/L_{\text{OUV}}(t) = \text{const}$
- $\dot{M}_{*,\text{peak}}/L_{\text{Edd}} = 100$
- Efficient energy dissipation to CRs: $\epsilon_{\text{diss}} \simeq 0.2$
- Proton diffusion in Bohm regime $D = R_L c$



EM cascade spectra of AT2019dsg: M-IR (dust echo)

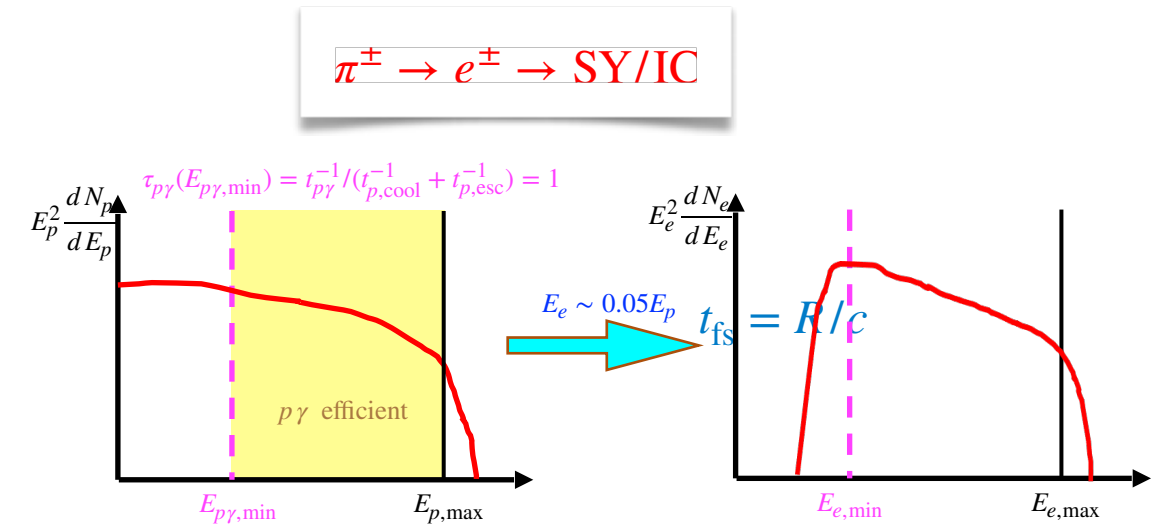
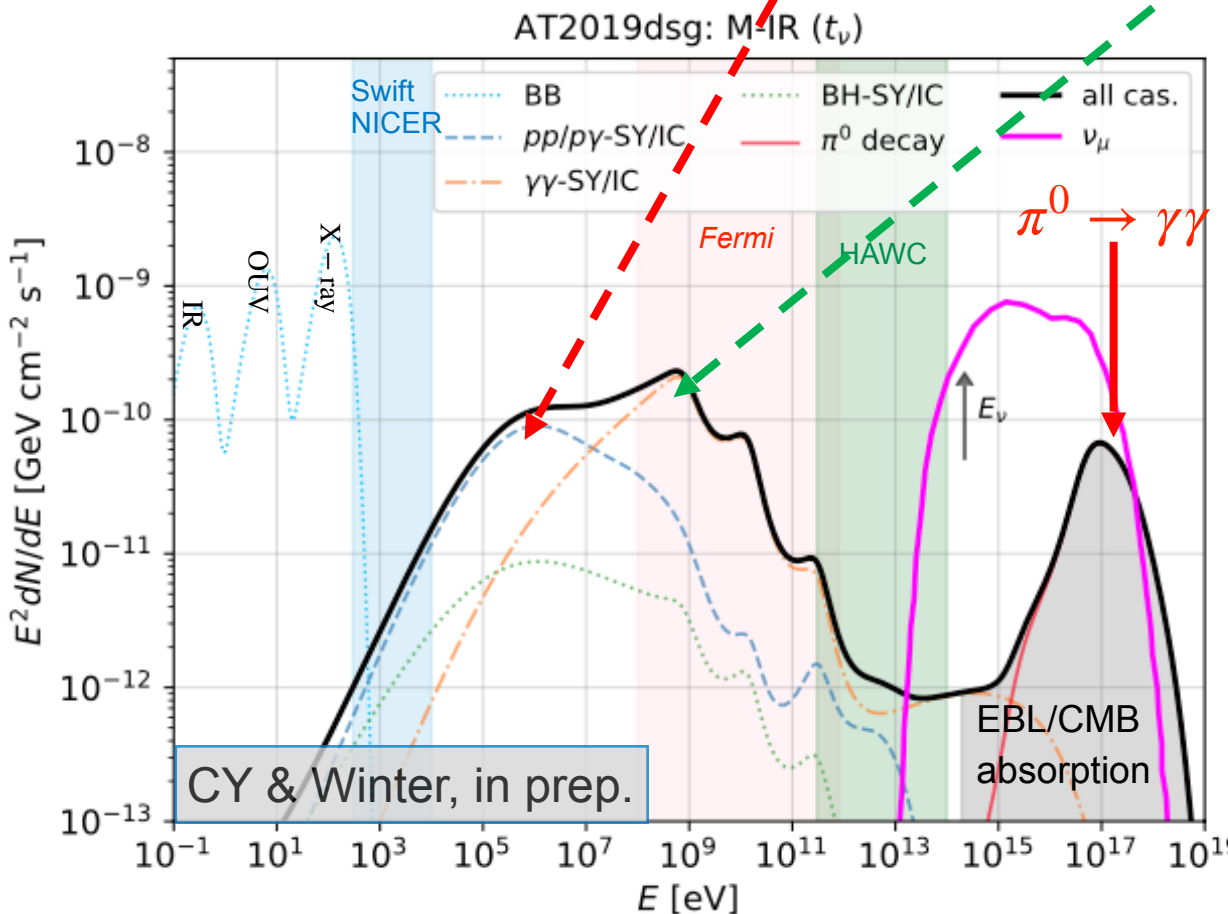
$p\gamma$ optically thin $t_{p\gamma}^{-1}/t_{fs}^{-1} < 1$: $(\pi^\pm \rightarrow e^\pm \rightarrow SY/IC) + (\gamma\gamma \rightarrow e^\pm \rightarrow SY/IC)$



Neutrino peak energy is significantly higher than the detected energy (green area) \rightarrow low N_ν

EM cascade spectra of AT2019dsg: M-IR (dust echo)

$p\gamma$ optically thin $t_{p\gamma}^{-1}/t_{fs}^{-1} < 1$: $(\pi^\pm \rightarrow e^\pm \rightarrow SY/IC) + (\gamma\gamma \rightarrow e^\pm \rightarrow SY/IC)$



$$E_{pp/p\gamma,SY} \sim \frac{3}{4\pi} h \gamma_{e,\min}^2 \frac{eB}{m_e c}$$

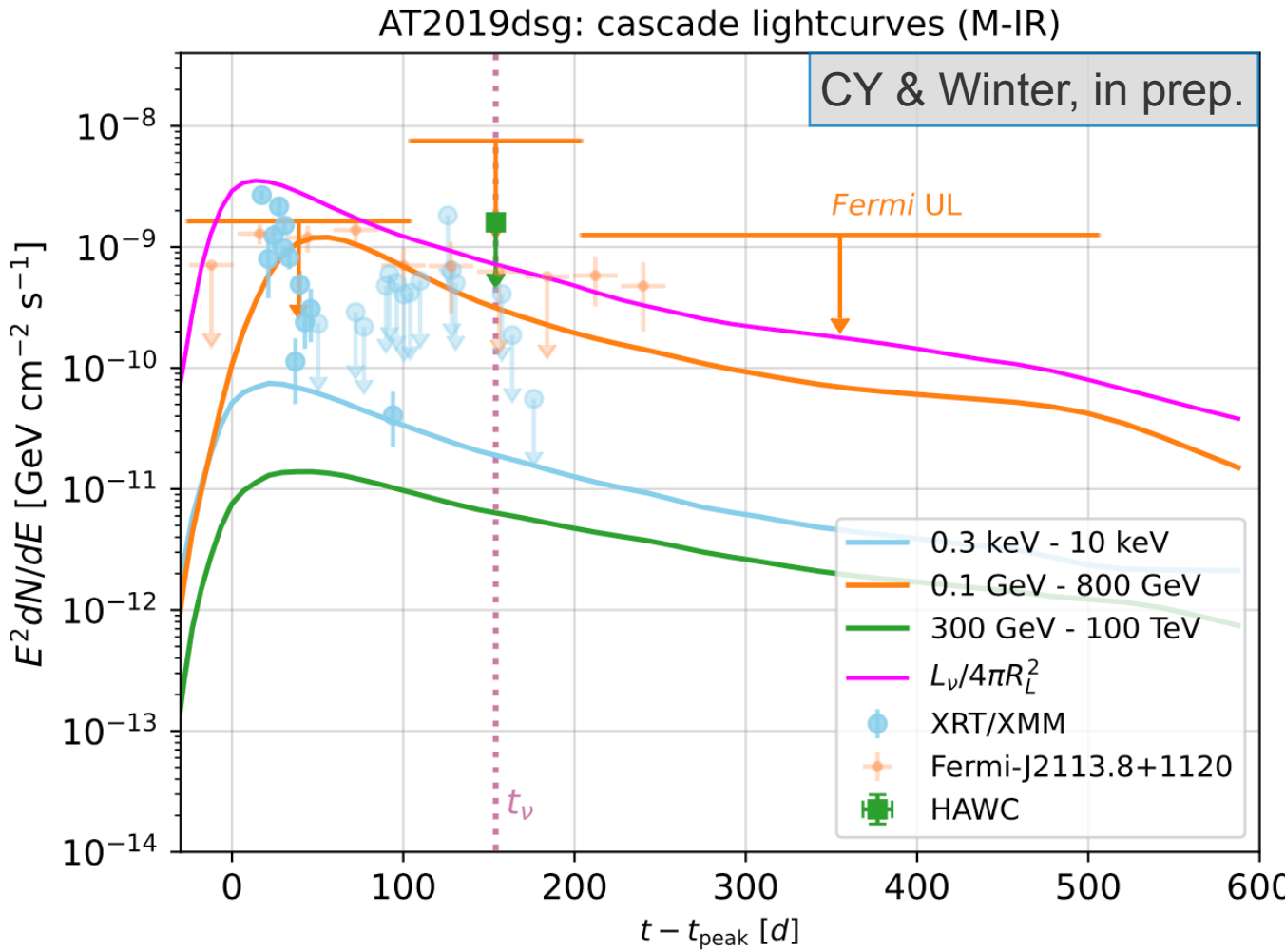
$$\sim 420 B_{-1} \left(\frac{E_{p\gamma,\min}}{10^5 \text{ GeV}} \right)^2 \text{ keV}$$

$\gamma\gamma$ absorption

$$E_\gamma \sim m_e^2/E_{bb} \simeq 2 \text{ GeV} (E_{bb}/100\text{eV})^{-1}$$

AT2019dsg Temporal signatures: M-IR

Dust echo scenario: $\epsilon_{\text{diss}} = 0.2$, $B = 0.1$ G, $R = 5 \times 10^{16}$ cm, $E_{p,\text{max}} = 5 \times 10^9$ GeV



Fermi-LAT uplimit (0.1 – 800 GeV)

Interval	MJD Start	MJD Stop	UL [$\text{erg cm}^{-2} \text{s}^{-1}$]
G1	58577	58707	2.6×10^{-12}
G2	58707	58807	1.2×10^{-11}
G3	58577	58879	2.0×10^{-12}

Extended Data Fig. 7 | Gamma-ray energy flux upper-limits for AT2019dsg. The values are derived assuming a point-source with power-law index $\Gamma=2.0$ at the position of AT2019dsg, integrated over the analysis energy range 0.1–800 GeV.

Stein et al. 2021

Consistent with Fermi UL., but predicts a low neutrino number

~50 days time delay is compatible with $p\gamma$ interaction time $t_{p\gamma} \sim 10 - 100$ d

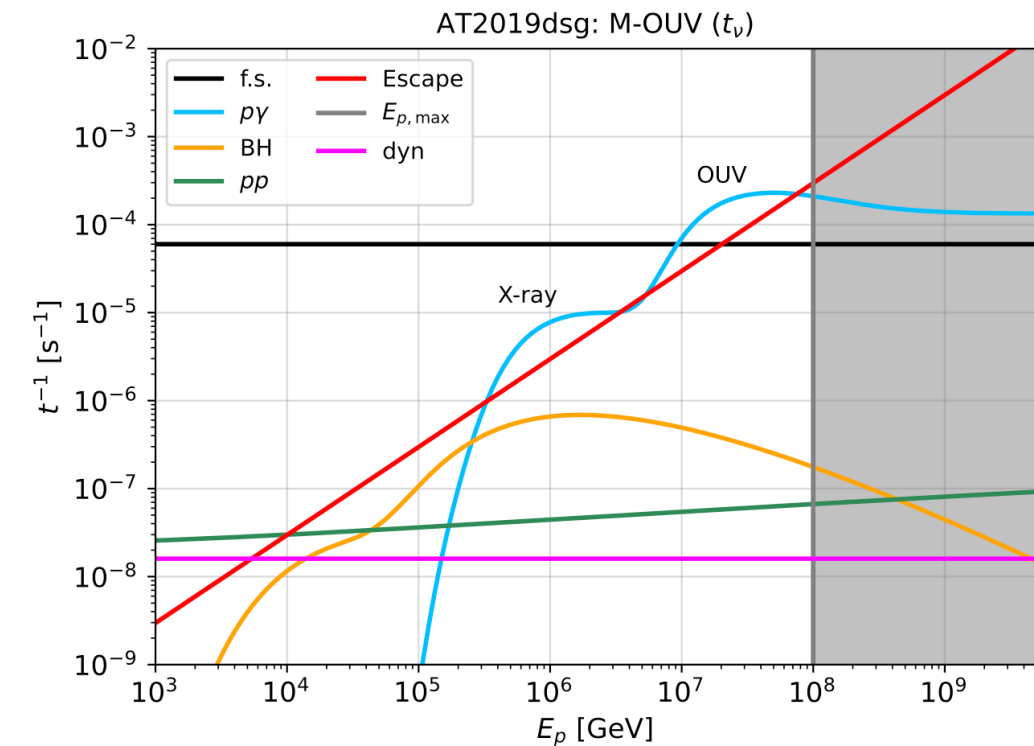
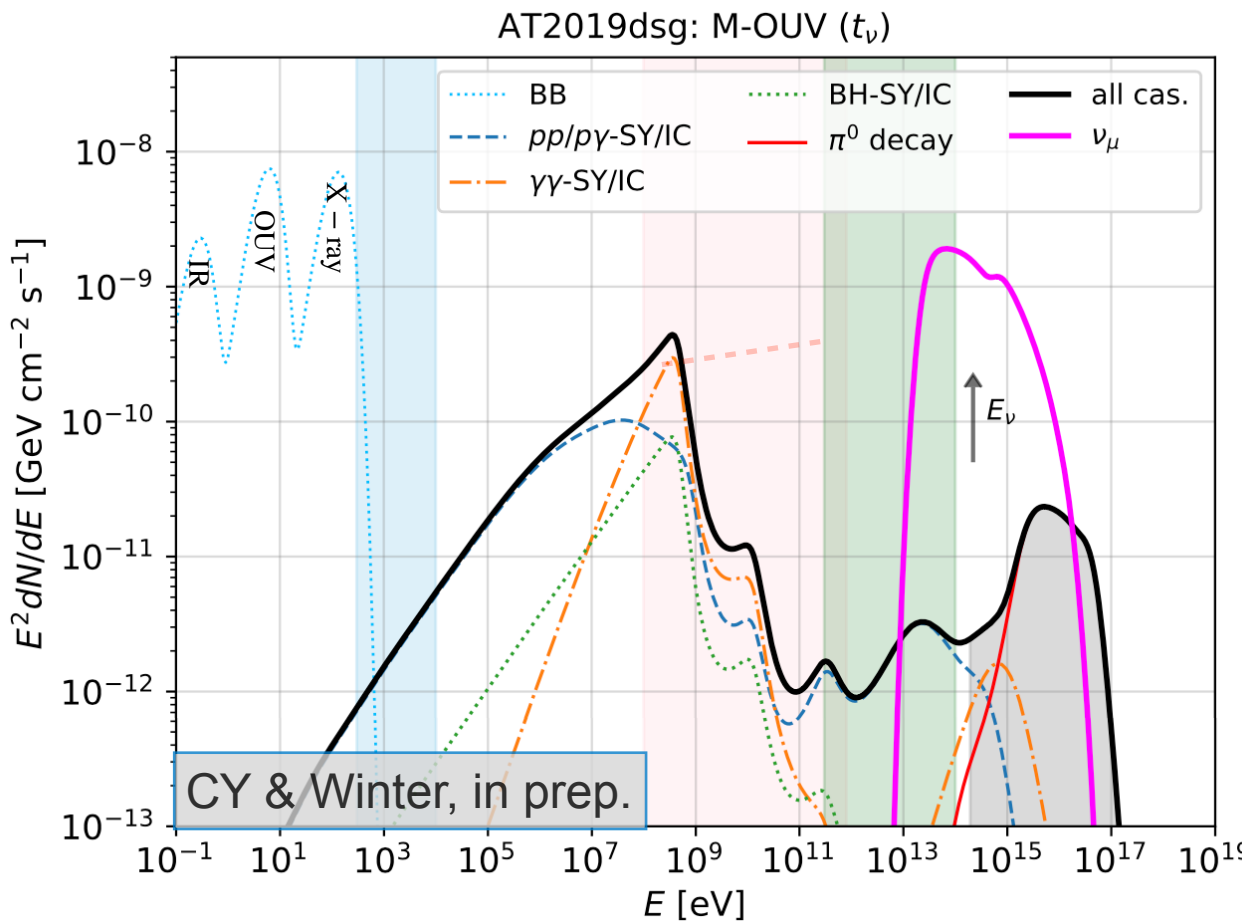
EM cascade spectra of AT2019dsg: M-OUV

$p\gamma$ optically thick $t_{p\gamma}^{-1}/t_{\text{fs}}^{-1} > 1$: $(\pi^\pm \rightarrow e^\pm \rightarrow \text{SY/IC}) + (\gamma\gamma \rightarrow e^\pm \rightarrow \text{SY/IC})$

Parameters: $\varepsilon_{\text{diss}} = 0.2$

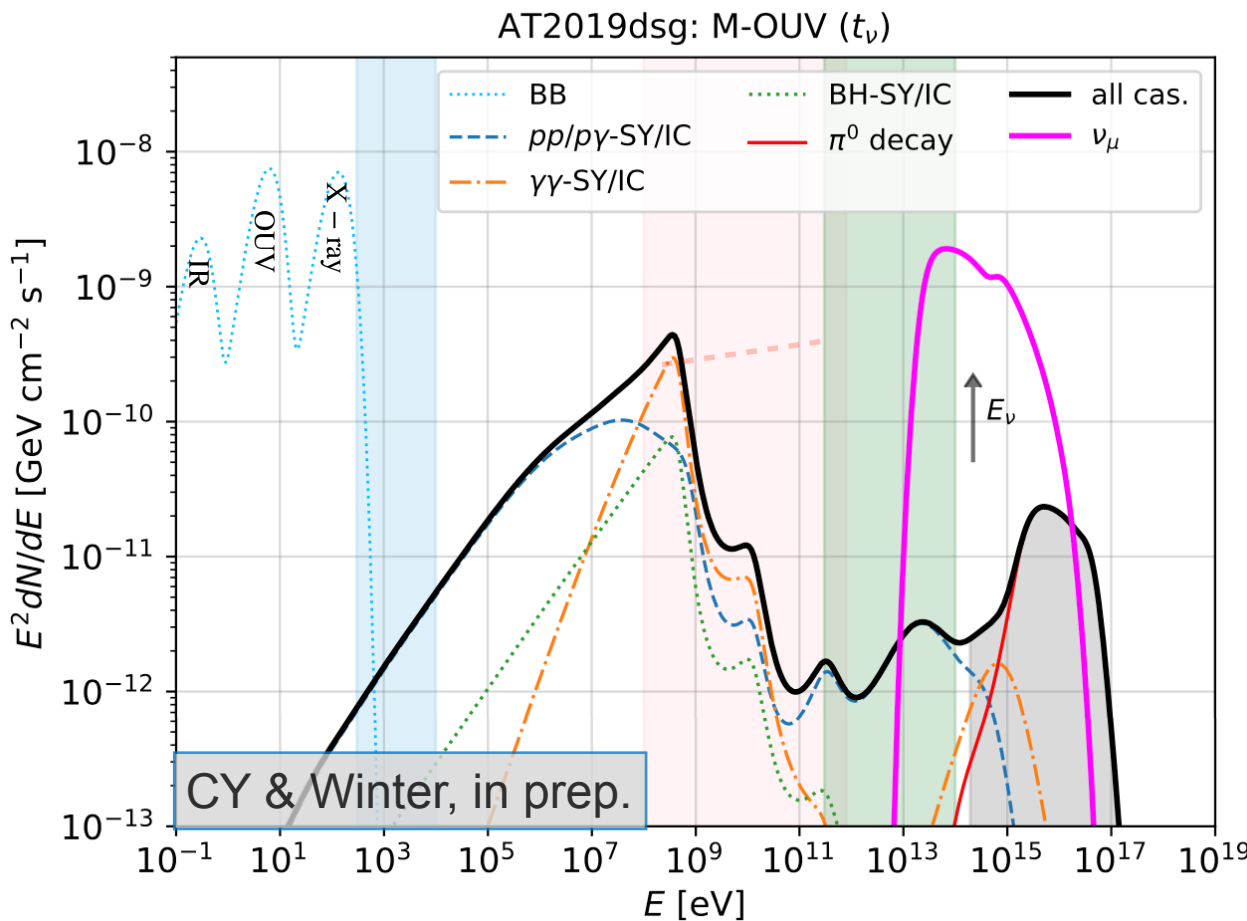
$B = 0.1$ G, $R = 5 \times 10^{14}$ cm, $E_{p,\text{max}} = 1 \times 10^8$ GeV

$R_{IR} \gg R \rightarrow$ IR subdominant ($n \propto L_{IR} R^{-2} c^{-1}$)



EM cascade spectra of AT2019dsg: M-OUV

$p\gamma$ optically thick $t_{p\gamma}^{-1}/t_{\text{fs}}^{-1} > 1$: $(\pi^\pm \rightarrow e^\pm \rightarrow \text{SY/IC}) + (\gamma\gamma \rightarrow e^\pm \rightarrow \text{SY/IC})$



Parameters: $\varepsilon_{\text{diss}} = 0.2$

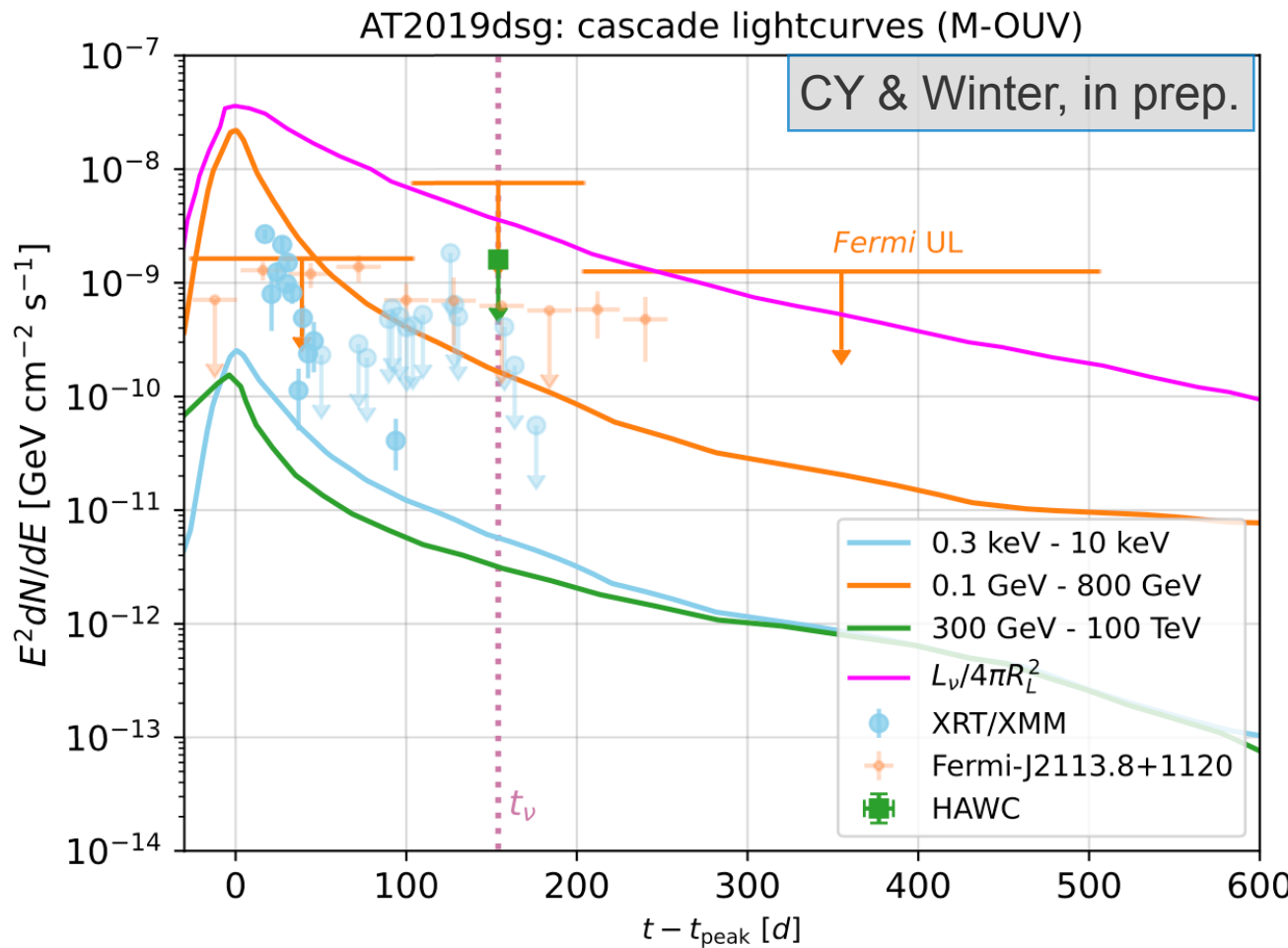
$B = 0.1 \text{ G}$, $R = 5 \times 10^{14} \text{ cm}$, $E_{p,\text{max}} = 1 \times 10^8 \text{ GeV}$

$R_{IR} \gg R \rightarrow$ IR subdominant ($n \propto L_{IR} R^{-2} c^{-1}$)

- Small R leads to fast proton escape
- $E_{p\gamma,\text{min}} \sim 10^{6-7} \text{ GeV}$
- Synchrotron peak energy $>$ GeV
- Attenuated before reaching the peak \rightarrow spikes
- Promising neutrino emitter in the neutrino energy range

AT2019dsg Temporal signatures: M-OUV

Compact region: $\epsilon_{\text{diss}} = 0.2$, $B = 0.1$ G, $R = 5 \times 10^{14}$ cm, $E_{p,\text{max}} = 1 \times 10^8$ GeV



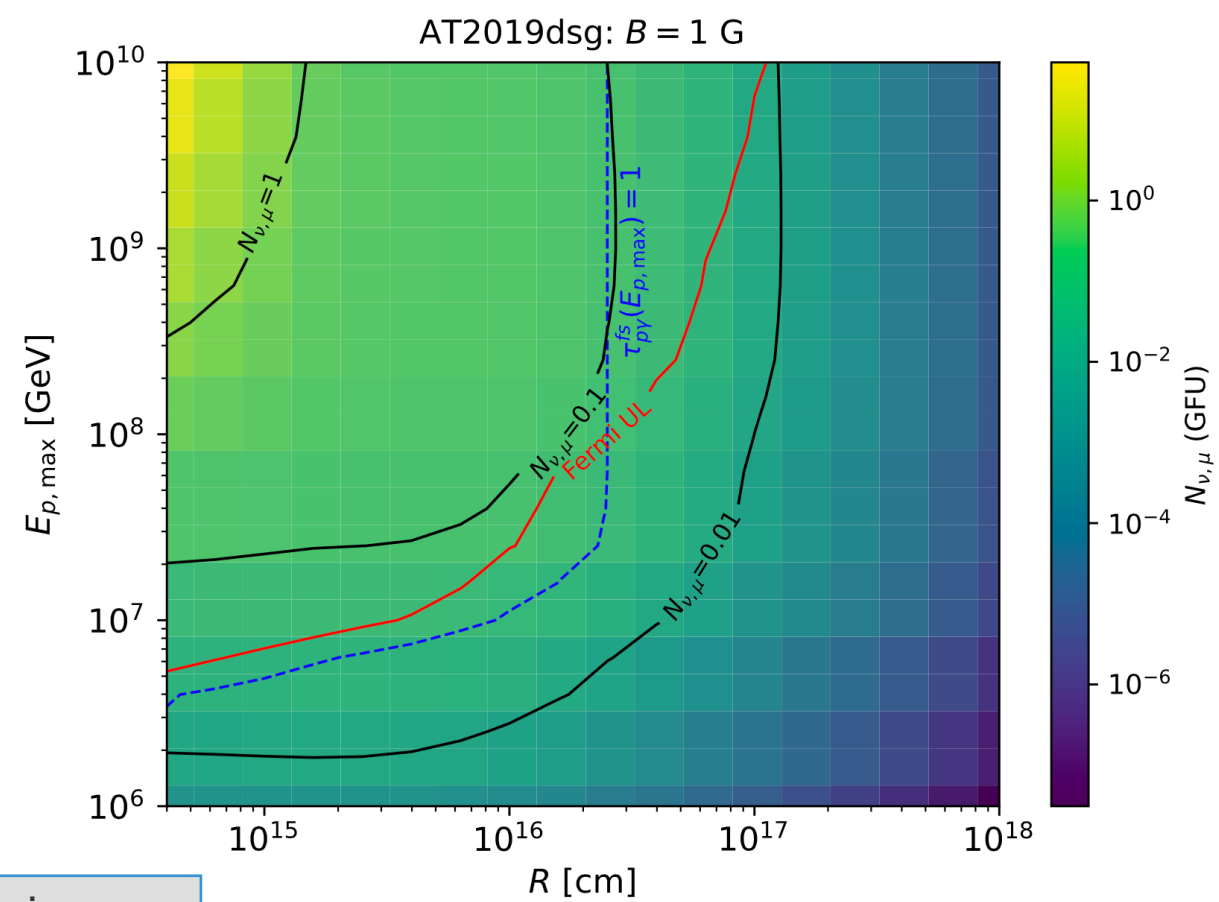
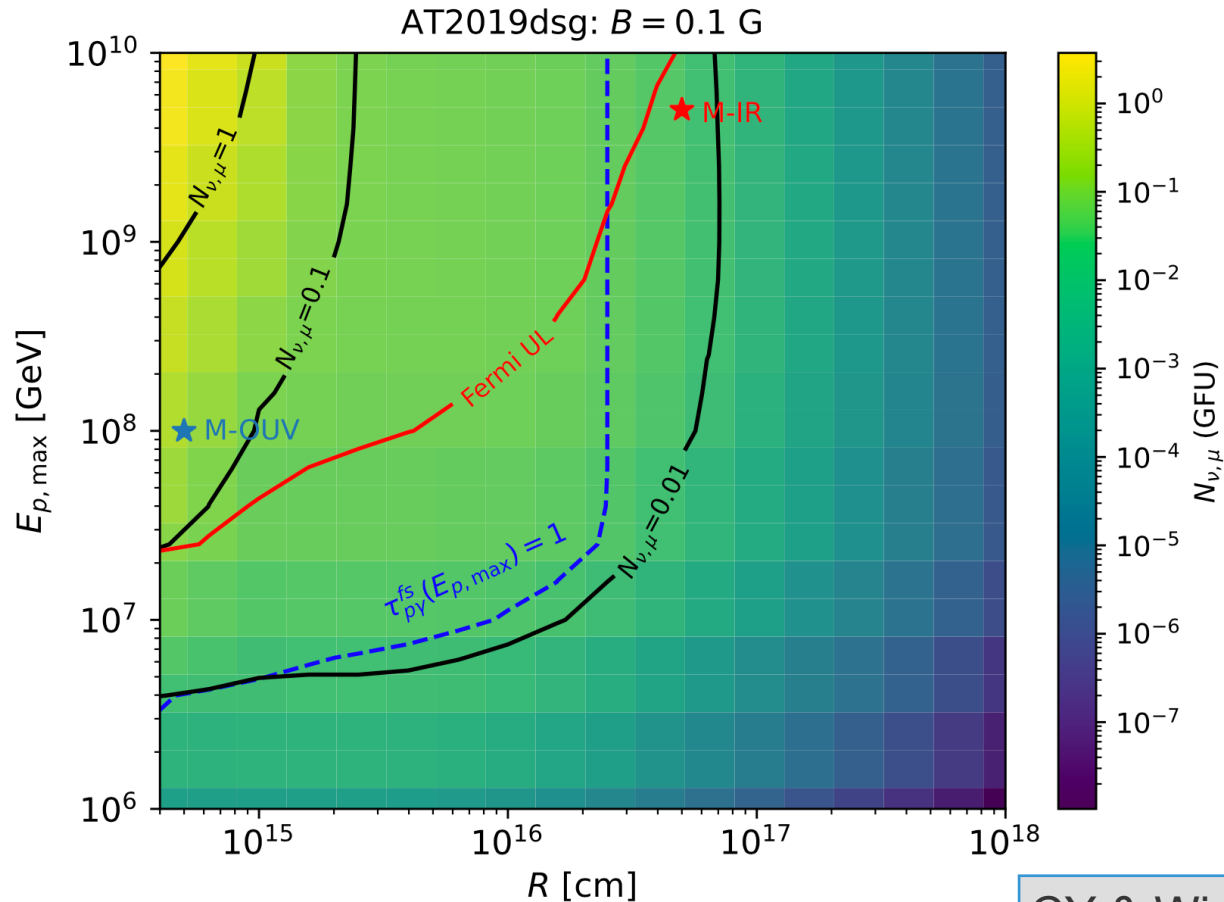
In this compact and dense region, interactions occur very fast

- $p\gamma$ optically thick: $t_{p\gamma}^{-1}/t_{\text{fs}}^{-1} > 1$
- Cascade emissions follows OUV light curve (no significant time delay)
- Cascade emission peaks in LAT energy range -> overshooting the γ -ray limits

Constraints on $E_{p,\max}$ and B

Obscured radiation region may be able to solve the missing γ -ray problem.

CRs are more confined with a stronger magnetic field, which enables a less compact region to be a promising neutrino emitter. (Easier to overshoot γ -ray up limits)



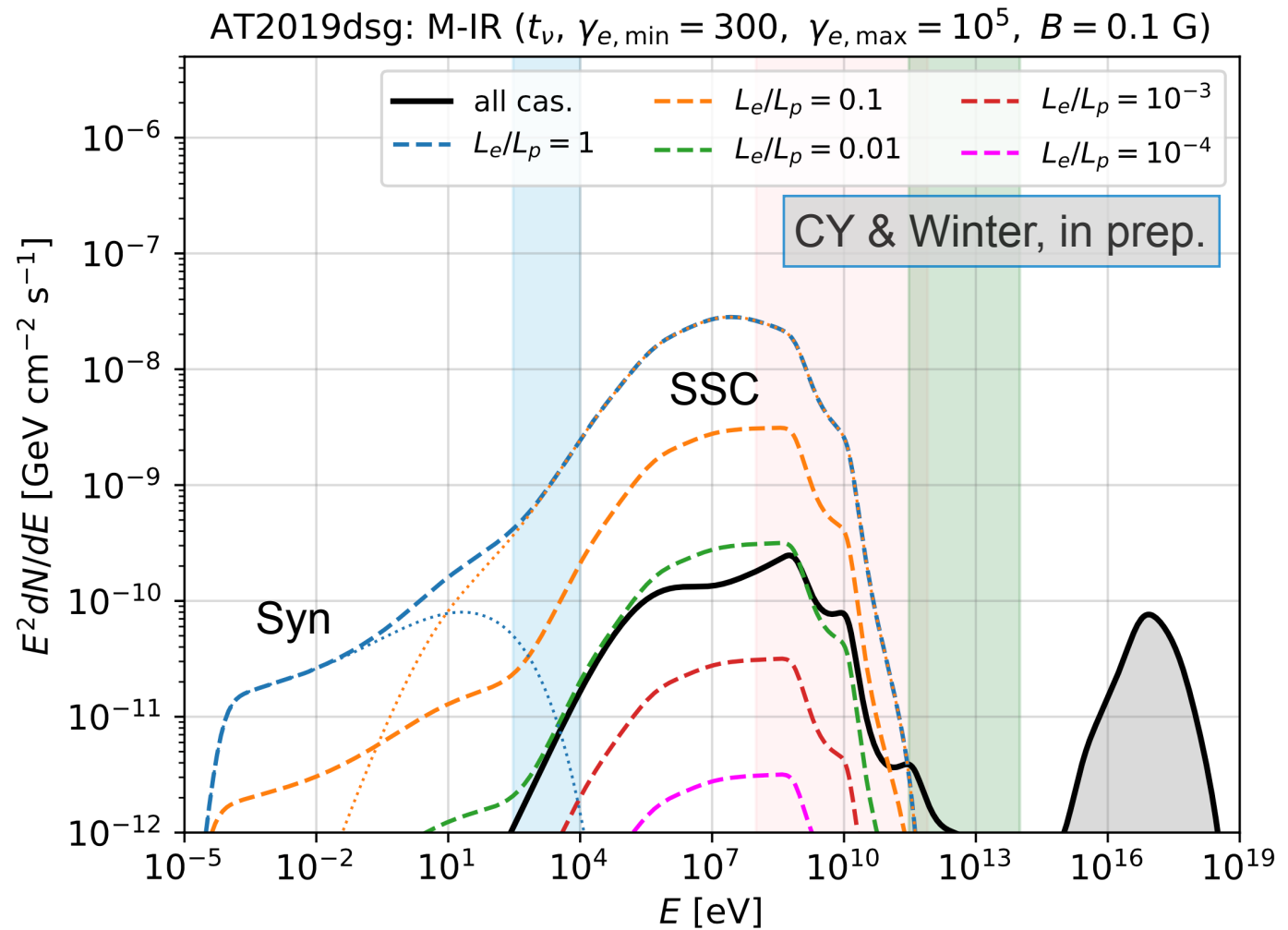
CY & Winter, in prep.

Test lepton (e^\pm) injections

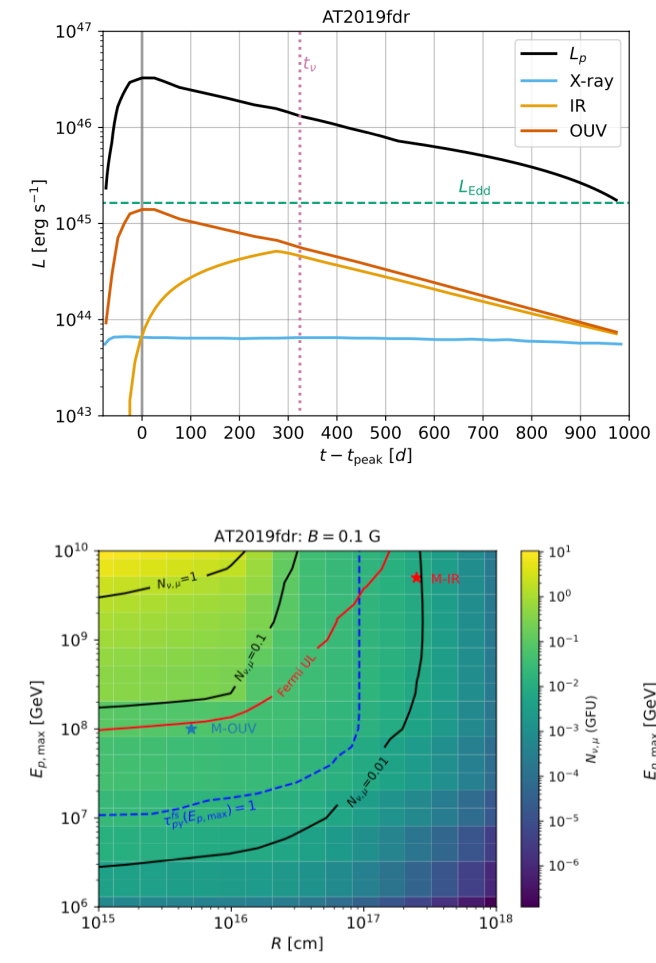
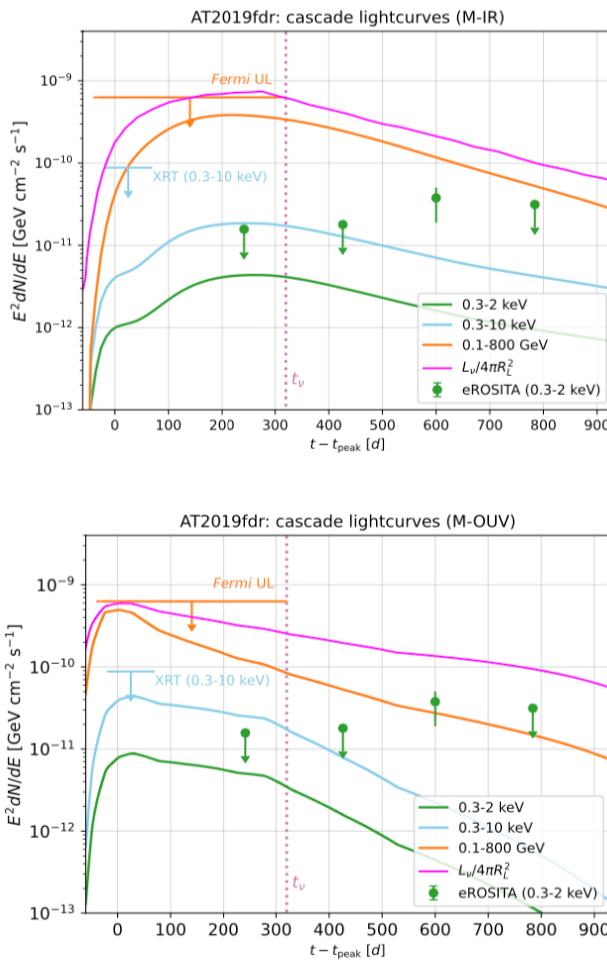
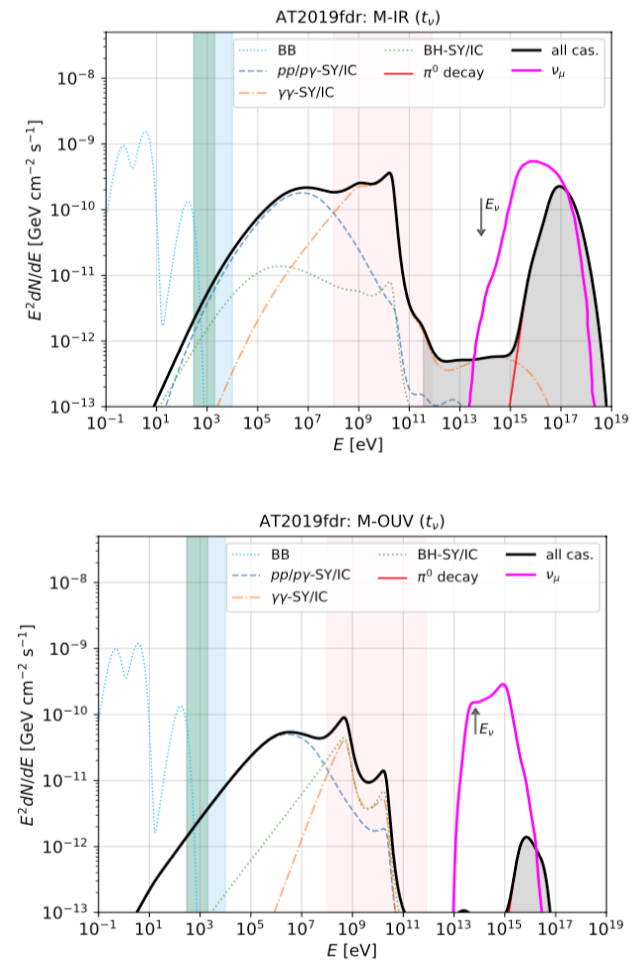
Electron injection spectra

- $dN_e/d\gamma_e \propto \gamma_e^{-2}$
- $\gamma_{e,\min} = 300$, $\gamma_{e,\max} = 10^5$ (typically used for AGNs)
- Magnetic field 0.1 G
- Lepton loading factor L_e/L_p varies from 10^{-4} to 1 (magenta to blue dashed lines).

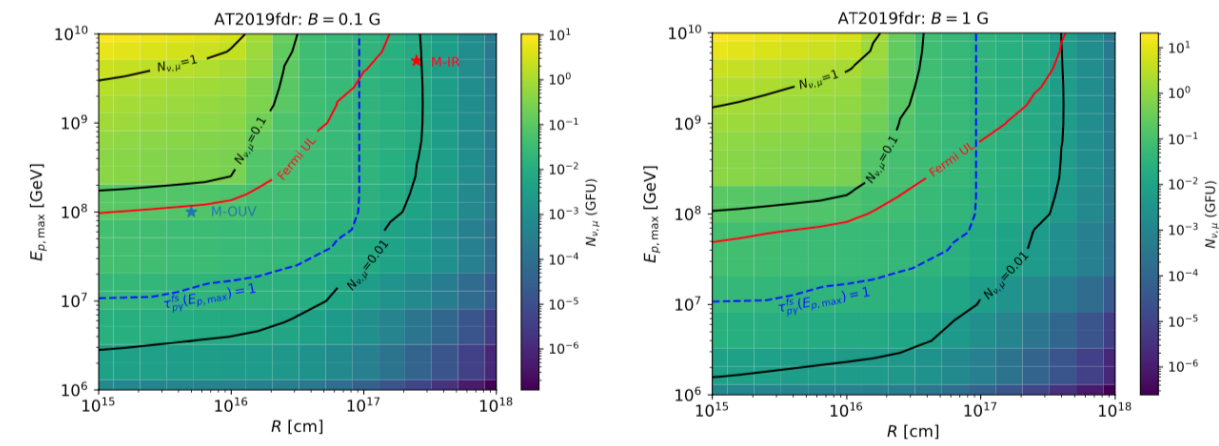
Cascade emission dominates if $L_e/L_p < 10^{-2}$



AT2019fdr



- $z = 0.267$
 $M_{\text{SMBH}} = 1.3 \times 10^7 M_{\odot}$
 $E_{\nu} = 82 \text{ TeV}$
- M-IR:**
- $R = 5 \times 10^{15} \text{ cm}$
 - $E_{p,\text{max}} = 10^8 \text{ GeV}$
- M-OUV:**
- $R = 2.5 \times 10^{17} \text{ cm}$
 - $E_{p,\text{max}} = 5 \times 10^9 \text{ GeV}$



CY & Winter, in prep.

Summary and outlook

- EM/hadronic cascade processes in TDE winds can produce detectable X-ray/ γ -ray emissions, e.g., M-IR (dust echo scenario). **But so far no γ -ray has been detected!**
- Significant (\sim 10-100 days) time delay is expected in the $p\gamma$ optically thin regime.
- To explain the neutrino coincidence, **very efficient energy dissipation to CRs and compact/dense radiation region** are needed. The accompanying cascade emission will **unavoidably overshoot the X-ray/ γ -ray constraints**.
- γ -ray obscured/hidden models may solve the missing γ -ray problem.
- It would be interesting to explore the time-dependent lepto-hadronic signatures in jetted TDEs, e.g., AT2022cmc, using jet-wind-cocoon models.
- TDEs as the origin of UHECRs?

Jet-induced electromagnetic and neutrino emission from SMBH mergers

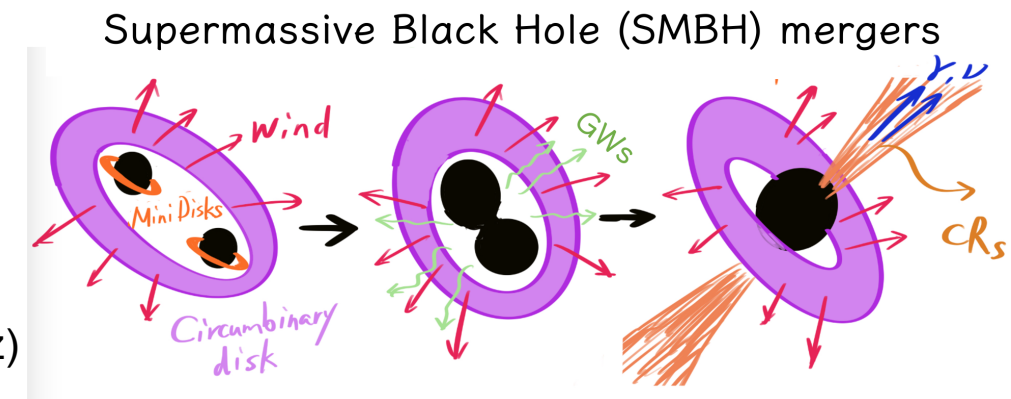
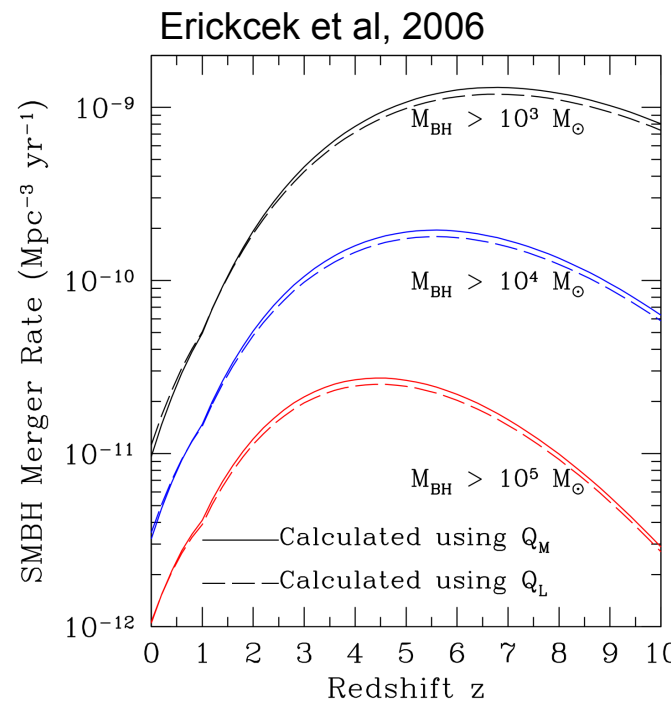
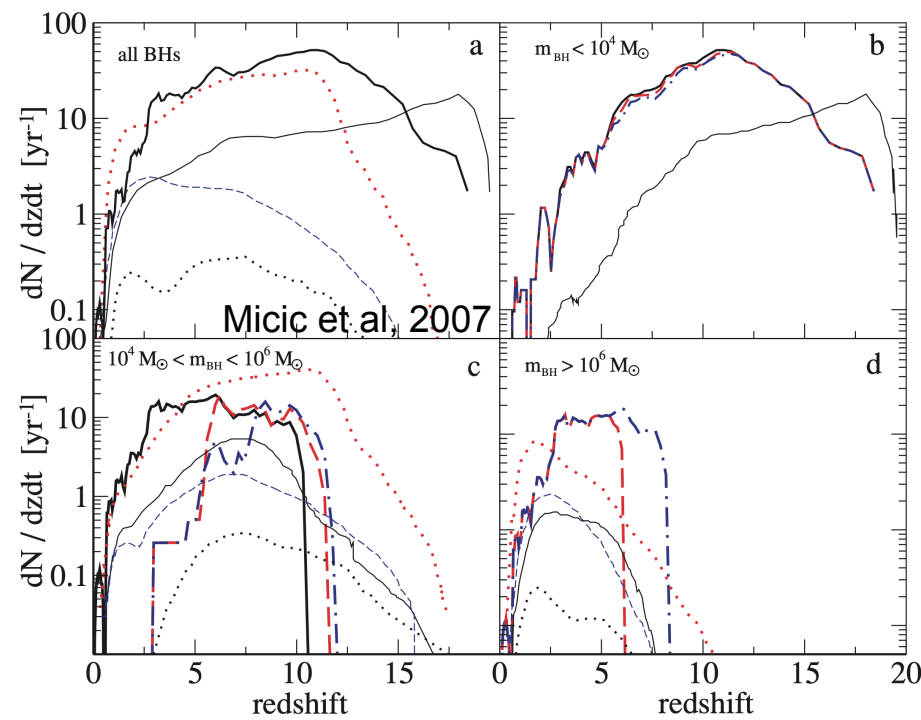
- Simulations and physical picture
- Post-merger Jet-cocoon-wind model
- GW-Neutrino detection perspectives
- EM counterparts

SMBH mergers

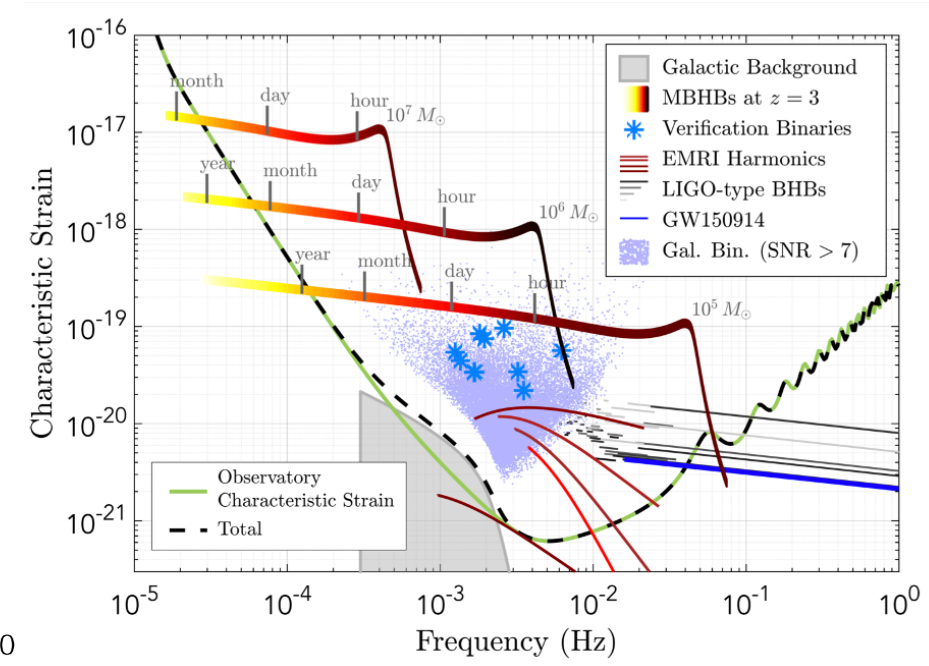
SMBHs can grow their mass via hierarchical mergers

(one influential theory for SMBH formation)

- The merger rate can be estimated from **halo merger history** (Erickcek et al, 2006) and **cosmological N-body simulations** (Micic et al, 2007)
- Coalescence will lead to a gravitational wave (GW) burst ($10^{-4} - 10^{-2}$ Hz) detectable by LISA
- Accretion activities may generate relativistic jets \rightarrow multimessenger signals



Laser Interferometer Space Antenna (LISA)

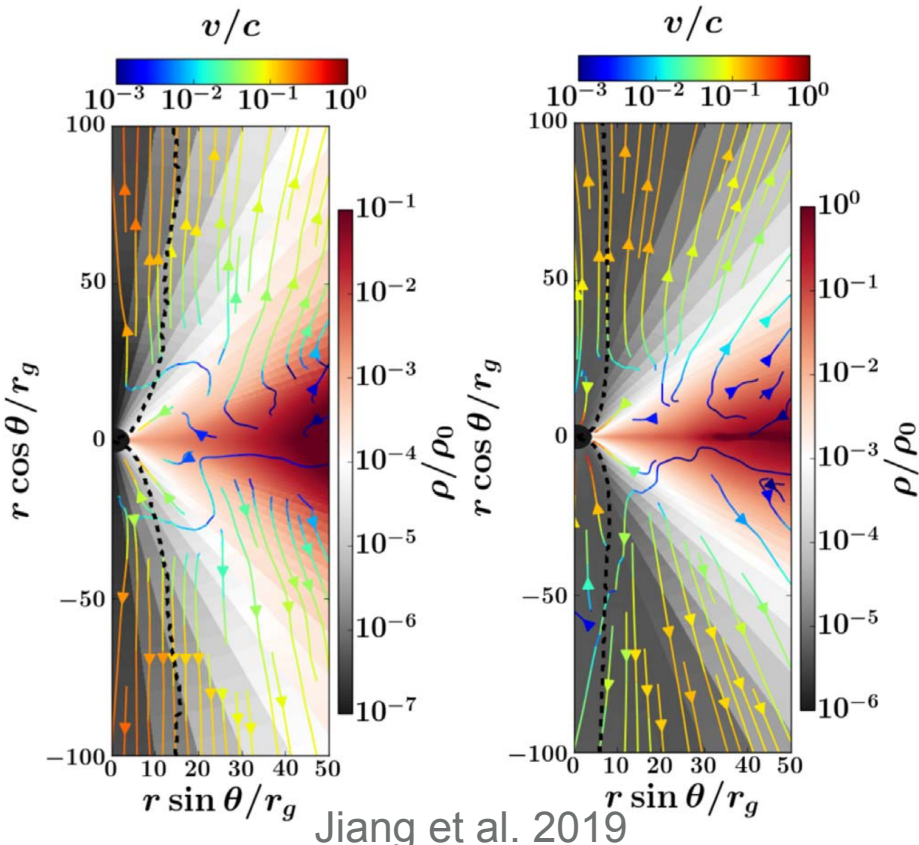


Credit: LISA collaboration proposal to the ESA

SMBH mergers: simulations

Azimuthally averaged spatial structure

- For super-Eddington case, up to $\eta_w = \dot{M}_w / \dot{M}_{\text{BH}} \sim 15\%$ of accreted mass can go to wind
- A few percent for sub-Eddington cases
(e.g., Ohsuga et al, 2009, Jiang et al 2019,)

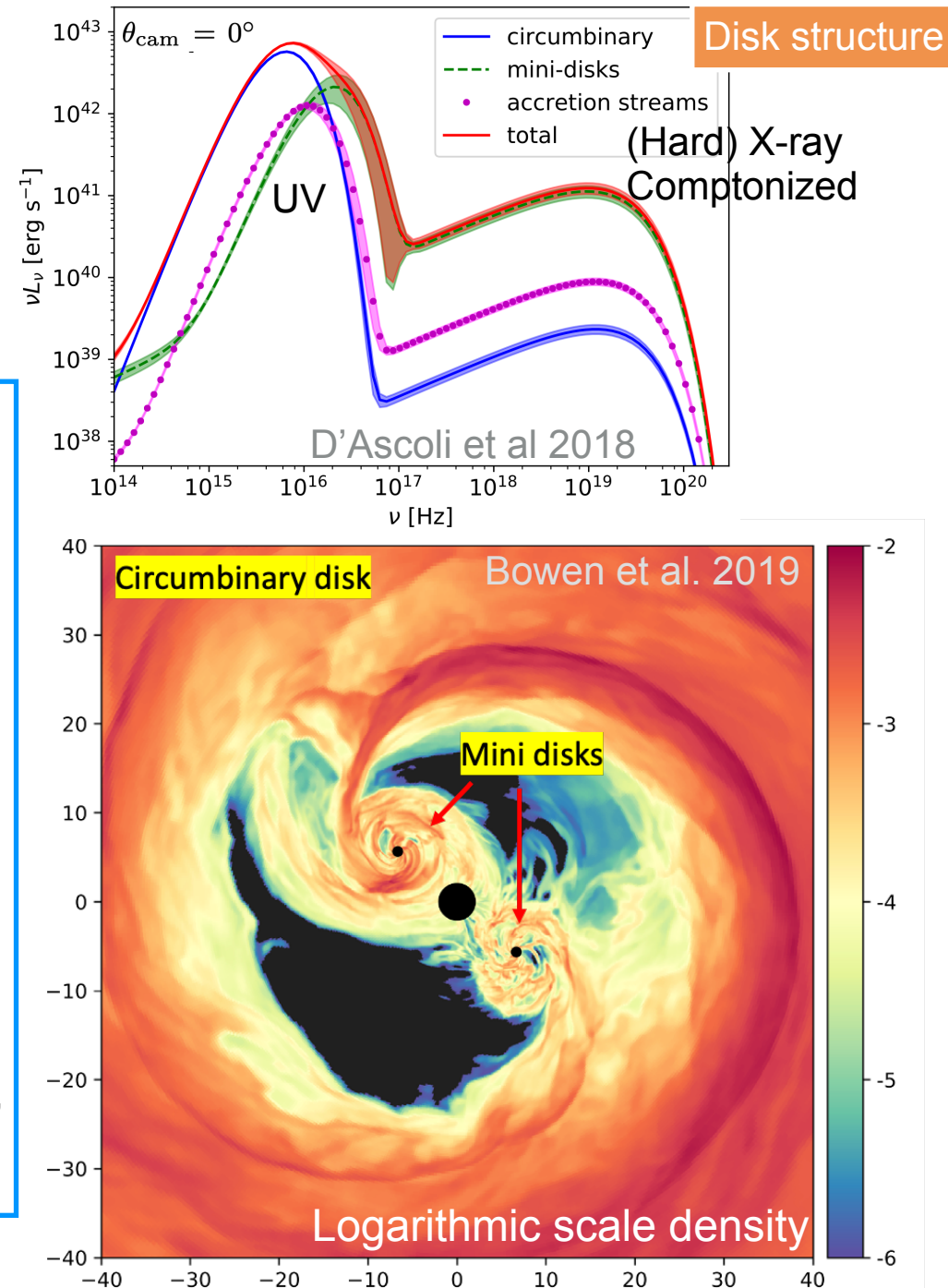


Rotation energy can be extracted via poloidal magnetic fields: **Blandford–Znajek mechanism**

Accretion onto spinning BHs can generate relativistic jets
(Sadowski et al. 2014)



Particle acceleration, non-thermal EM emission, neutrinos



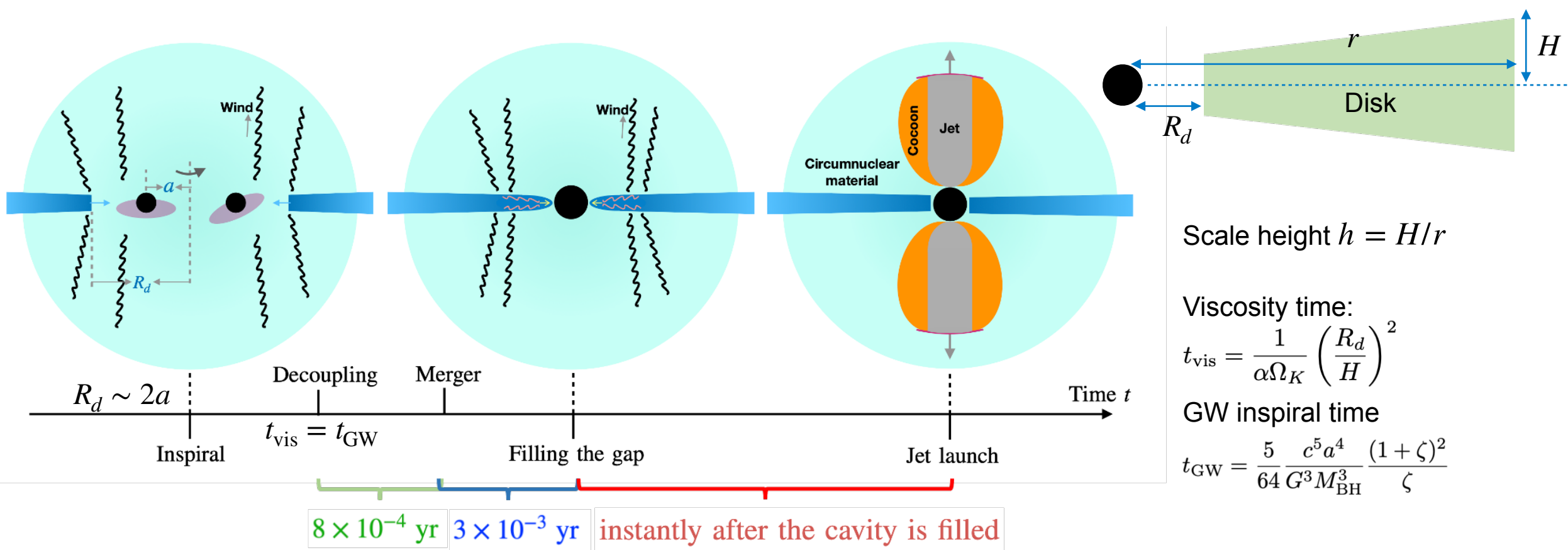
SMBH mergers: physical picture

Yuan, Murase, Kimura, Meszaros 20 PRD 102.083013

Merger \rightarrow circumnuclear gas bubble (wind) + jet (BZ mechanism) \rightarrow internal, collimation, forward and reverse shocks \rightarrow VHE CRs, PeV neutrinos

Time lag between GW burst and jet launch: 10^{-3} - 10^{-2} yr

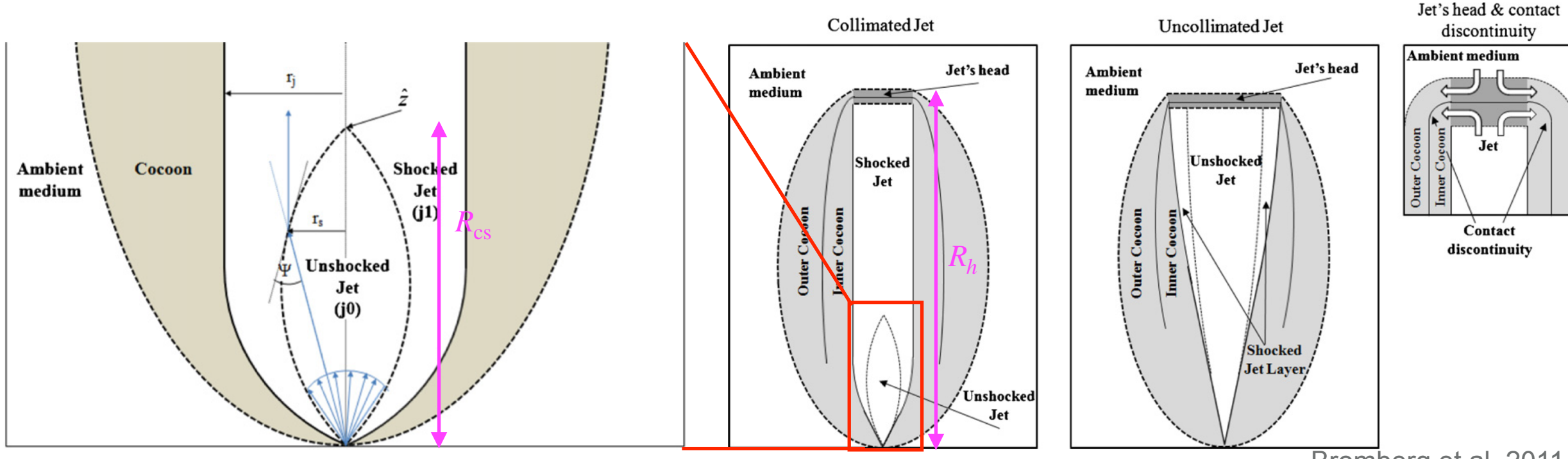
Scaleheight $h = 0.01$ (thin disk) – 0.3(thick disk)



Post-merger jets: collimation condition

When a conical jet propagates into the medium [gas/wind envelope] of density $\rho_w = \eta_w(1 + \chi)\dot{M}_{\text{BH}}/(4\pi v_w r^2)$ (χ counts for the mini-disk contribution, $\eta_w = \dot{M}_w/\dot{M}_{\text{BH}}$)

- Jet head (forward shock, reverse shock), cocoon, and collimation shock will be formed
- The jet will be collimated to cylindrical shape if wind is dense enough
- Collimation condition $R_h > R_{\text{cs}}$



Bromberg et al, 2011

Post-merger jet structure

Jet-cocoon-wind model:

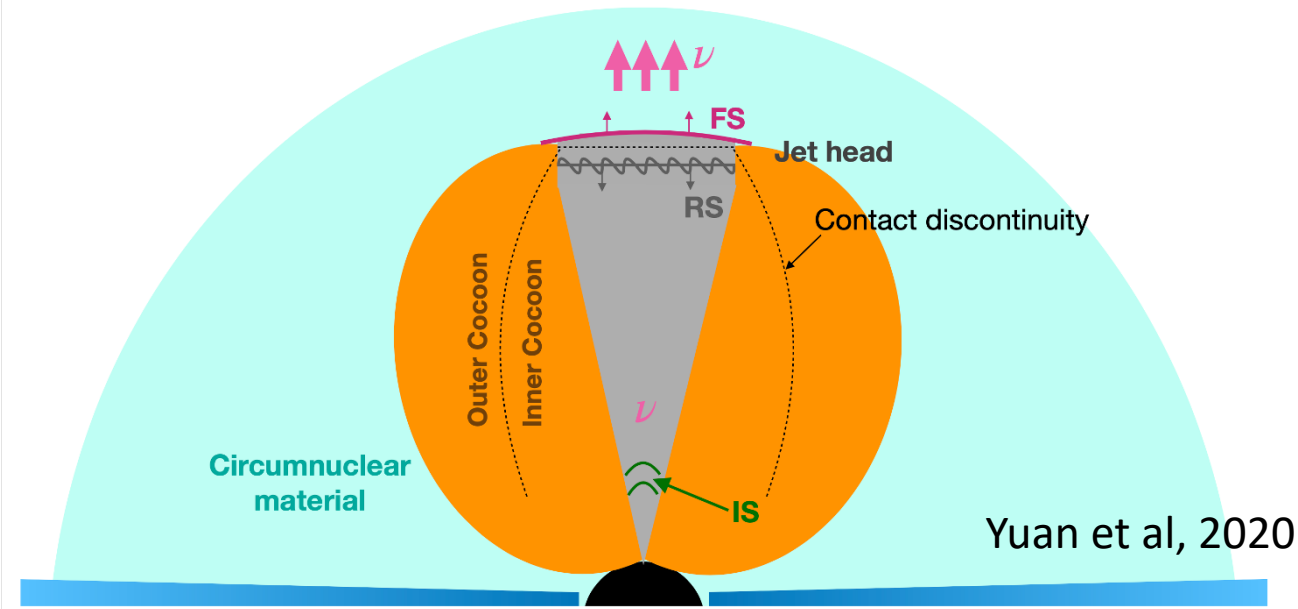
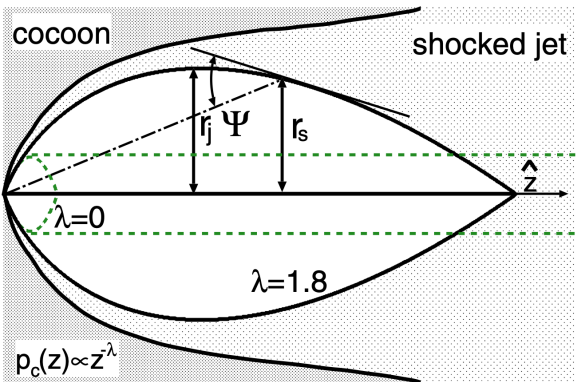
Balancing the ram pressure applied on the FS and RS ($\xi_c = \xi_w = 1$ for wind profile, $\xi_w = \hat{\rho}_w/\rho_w \sim 3$)

$$R_h = \left(\frac{16}{3\pi} \frac{\tilde{\eta} \xi_w \xi_h^4}{\xi_c^2} \right)^{1/5} t_j^{3/5} L_{k,j}^{1/5} \varrho_w^{-1/5} \theta_j^{-4/5},$$

Balancing the jet and cocoon pressure yields

$$R_{cs} = \left(\frac{6}{\pi^{3/2}} \frac{\xi_h \xi_c^2}{\tilde{\eta} \xi_w} \right)^{1/5} t_j^{2/5} L_{k,j}^{3/10} c^{-1/2} \varrho_w^{-3/10} \theta_j^{-1/5}.$$

Parameter $\tilde{\eta} \sim 0.01$ is determined by simulations
(Mizuta & Ioka 2013)



The jet is uncollimated in our model:

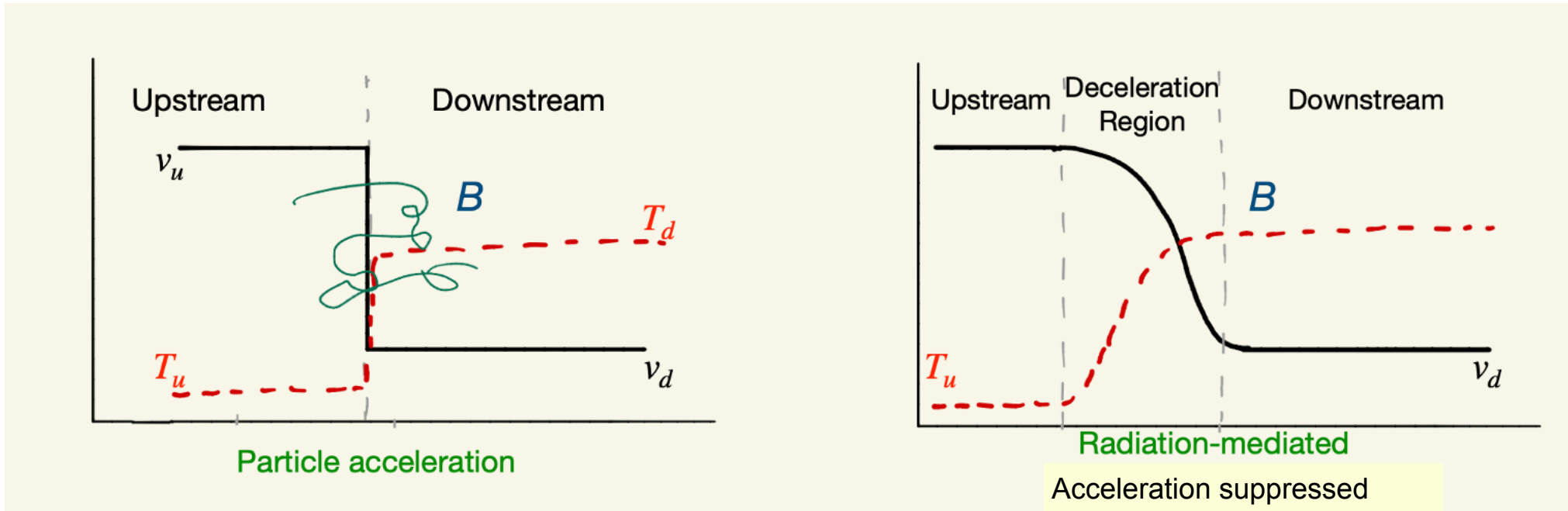
(optimistic case, super-Eddington)

- $M_{BH} = 10^6 M_\odot$
- $\dot{M}_{BH}/\dot{M}_{Edd} = 10$, $L_{k,j} \sim \dot{M}_{BH} c^2$, $\theta_j \simeq 0.1$, $\eta_w \sim 0.01$
- $R_h > R_{cs}$ cannot be achieved
- Jet head Lorentz factor $\Gamma_h \sim \tilde{L}^{1/4}/\sqrt{2} \simeq 3$, $\tilde{L} = P_j/P_w$
- Internal shock (IS) is formed by the fluctuation of unshocked materials and collision of fast/slow shells
- Three sites for neutrino production: FS, RS, IS

Radiation constraints and onset time

Conditions for particle acceleration

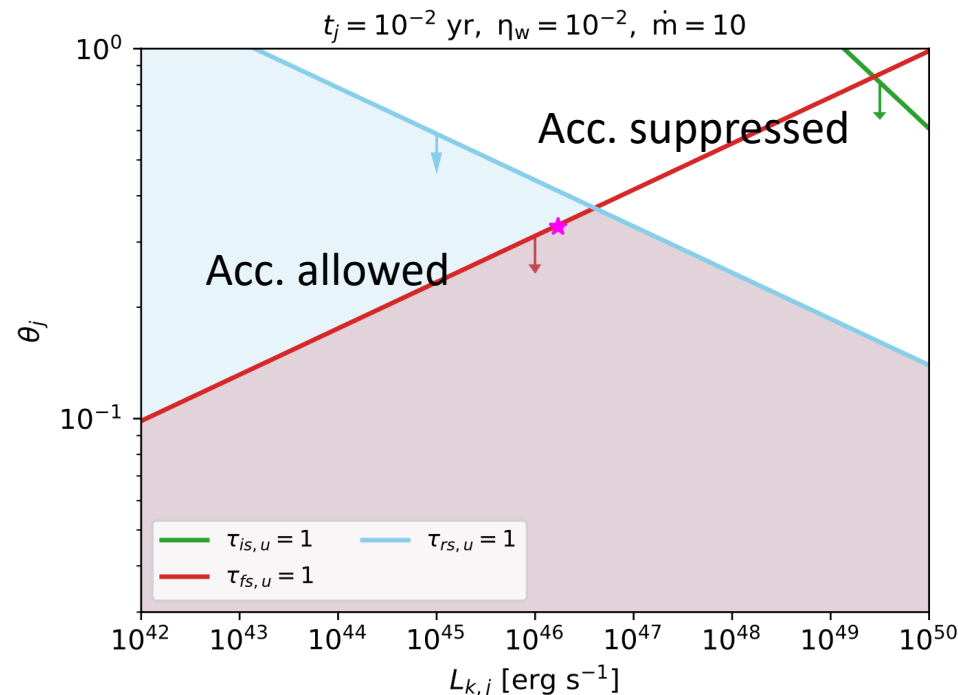
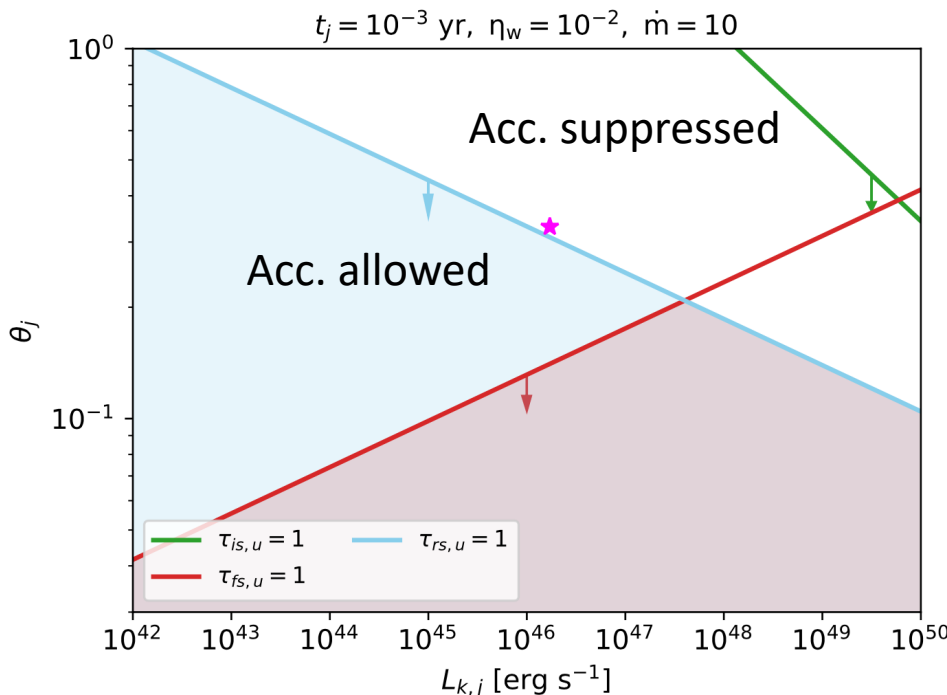
- Shock is **NOT radiation-mediated (optically thin upstream)** -> strong discontinuity/no energy lose -> efficient acceleration
$$\tau_u = n_u \sigma_T l_u \lesssim \min[1, \Pi(\Gamma_{\text{sh}})]$$
- n_u comoving number density of upstream materials, l_u comoving length of upstream, Π : e^+/e^- enrichment



Radiation constraints and onset time

Conditions for particle acceleration

- Shock is **NOT radiation-mediated (optically thin upstream)** -> strong discontinuity/no energy lose -> efficient acceleration
$$\tau_u = n_u \sigma_T l_u \lesssim \min[1, \Pi(\Gamma_{\text{sh}})]$$
- Neutrino emission onset time t_* , defined by $\tau_u(t_*)=1$. (optically thin)**
- n_u comoving number density of upstream materials, l_u comoving length of upstream, Π : e^+/e^- enrichment

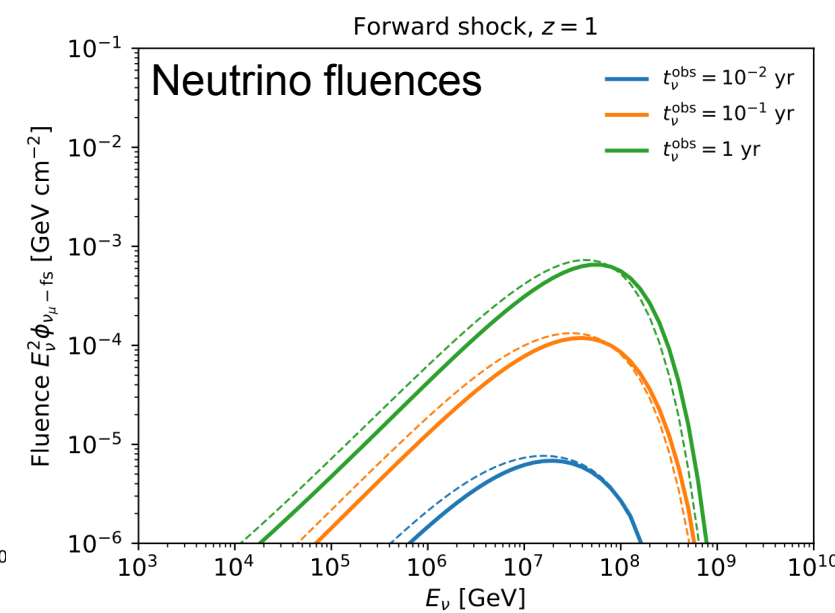
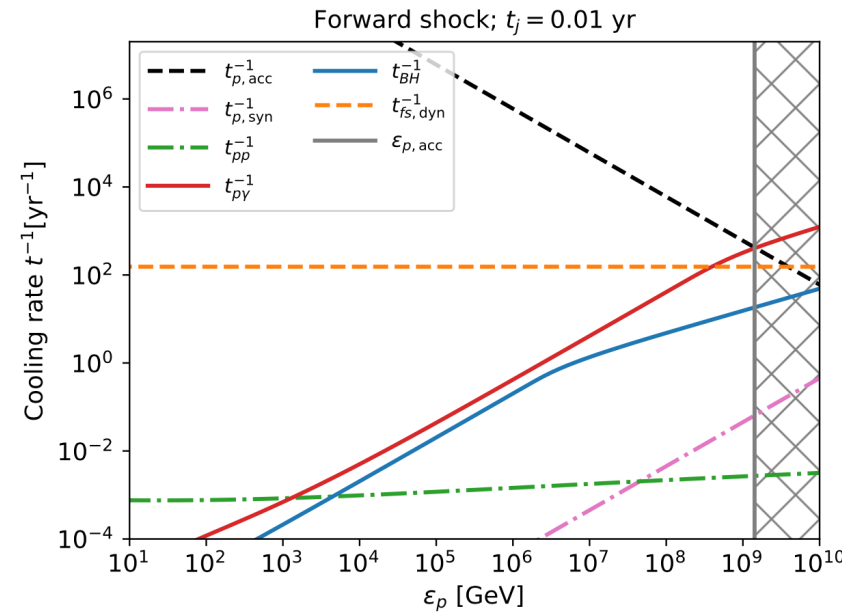
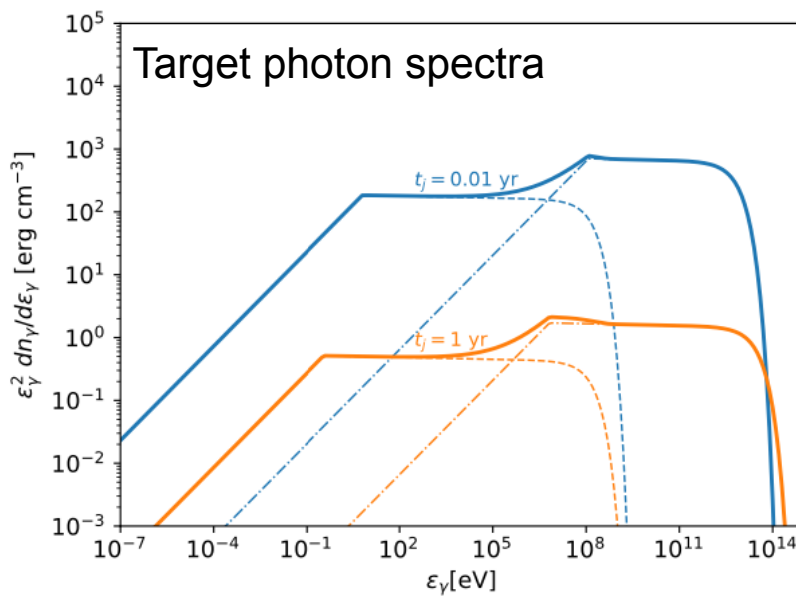


Yuan, Murase, Kimura, Meszaros 20 PRD 102.083013

Proton injection and neutrino production

Proton injection $dN_p/d\varepsilon_p \propto \varepsilon_p^{-2} \exp(-\varepsilon_p/\varepsilon_{p,\max})$

- Cooling processes: proton synchrotron, $p\gamma$, pp , BH
- Target proton: $n_{fs,u} = \rho_w/m_p$
- Target photon: electron synchrotron and synchrotron self-Compton ($L_e = \epsilon_e L_{k,j}$, $\epsilon_e = \epsilon_B = 0.01$, $B \propto \epsilon_B^{1/2} n_{is,u}^{1/2}$)
- $\varepsilon_{p,\max}$ is solved from $t_{p,\text{acc}}^{-1} = t_{p,\text{syn}}^{-1} + t_{p\gamma}^{-1} + t_{pp}^{-1} + t_{BH}^{-1}$,
 $t_{p,\text{acc}} \sim \varepsilon_p/(eBc)$



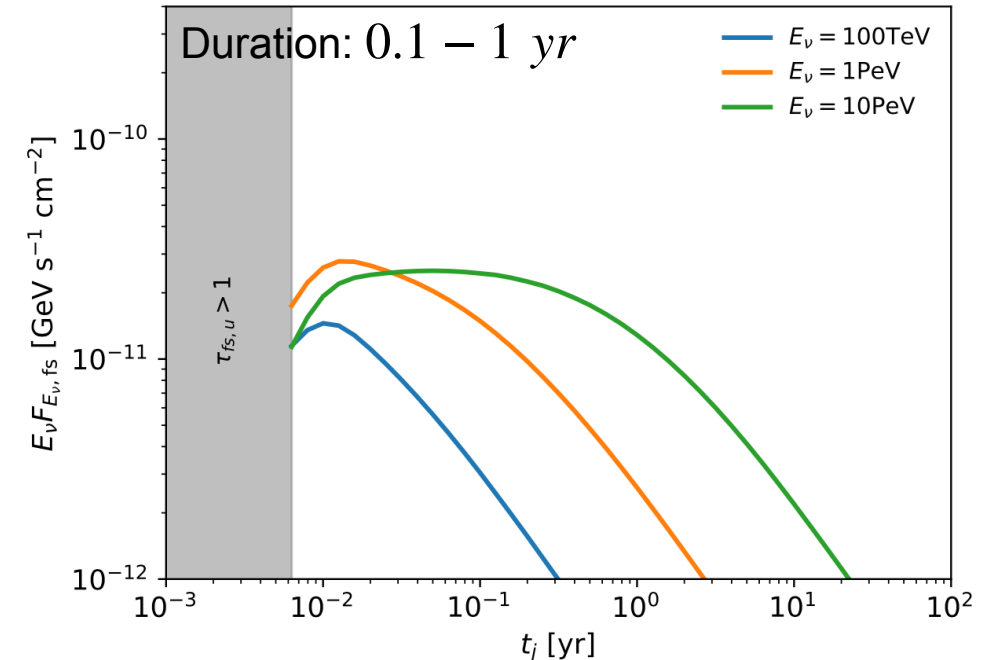
Neutrino-GW coincidence rate

Given the SMBH merger rate $\mathcal{R}(z)$, the neutrino detection rate [yr^{-1}] with in the redshift range $z < z_{\text{lim}}$

$$\begin{aligned}\dot{N}_{\nu,i}(< z_{\text{lim}}) &= \frac{c}{H_0} f_{b,i} \Delta\Omega_{\text{sur}} \\ &\times \int_0^{z_{\text{lim}}} dz \frac{P_{m \geq 1}(\mathcal{N}_i|t_{\nu}^{\text{obs}}=1 \text{ yr}) \mathcal{R}(z) d_L^2}{(1+z)^3 \sqrt{\Omega_m(1+z)^3 + \Omega_{\Lambda}}}\end{aligned}$$

The IceCube/IceCube-Gen2 neutrino detection number is calculated via

$$\mathcal{N}_i(t_{\nu}^{\text{obs}}) = \int \phi_{\nu_{\mu}-i} A_{\text{eff}}(\delta, E_{\nu}) dE_{\nu}$$



Neutrino detection rate $\dot{N}_{\nu,i}$ for SMBH mergers within the LISA detection range $z \lesssim 6 \text{ [yr}^{-1}]$

Scenario	Optimistic parameters			Conservative parameters		
	$\dot{m} = 10, L_{k,j} \simeq 3.4 \times 10^{46} \text{ erg s}^{-1}, \epsilon_p = 0.5, h = 0.3$	$\dot{m} = 0.1, L_{k,j} \simeq 3.4 \times 10^{44} \text{ erg s}^{-1}, \epsilon_p = 0.5, h = 0.01$	IC-Gen2 (up+hor)	IC (up+hor)	IC (down)	IC-Gen2 (up+hor)
IS	0.019	0.014	0.13	8.2×10^{-4}	4.3×10^{-4}	3.7×10^{-3}
FS	4.6×10^{-3}	2.8×10^{-3}	0.028	3.5×10^{-5}	2.9×10^{-5}	2.1×10^{-4}
RS	0.011	8.4×10^{-3}	0.044	9.6×10^{-5}	7.2×10^{-5}	4.1×10^{-4}

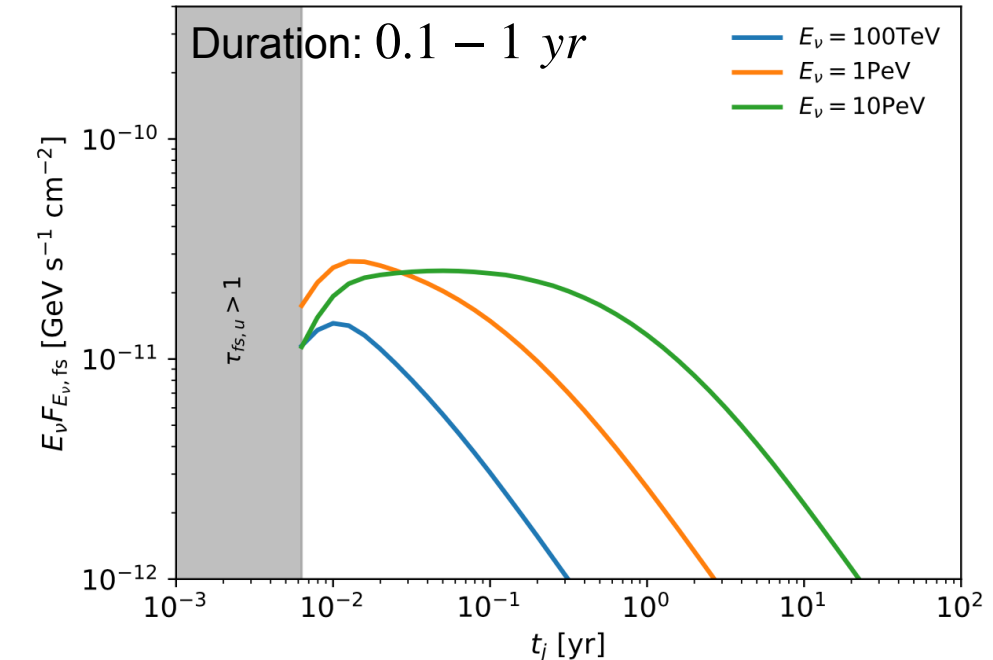
Neutrino-GW coincidence rate

Given the SMBH merger rate $\mathcal{R}(z)$, the neutrino detection rate [yr^{-1}] with in the redshift range $z < z_{\text{lim}}$

$$\begin{aligned} \dot{N}_{\nu,i}(< z_{\text{lim}}) &= \frac{c}{H_0} f_{b,i} \Delta\Omega_{\text{sur}} \\ &\times \int_0^{z_{\text{lim}}} dz \frac{P_{m \geq 1}(\mathcal{N}_i | t_{\nu}^{\text{obs}} = 1 \text{ yr}) \mathcal{R}(z) d_L^2}{(1+z)^3 \sqrt{\Omega_m(1+z)^3 + \Omega_{\Lambda}}} \end{aligned}$$

The IceCube/IceCube-Gen2 neutrino detection number is calculated via

$$\mathcal{N}_i(t_{\nu}^{\text{obs}}) = \int \phi_{\nu_{\mu}-i} A_{\text{eff}}(\delta, E_{\nu}) dE_{\nu}$$



Optimistic case (super-Edd.): IceCube Gen2 + LISA coincident
detection rate $\sim 1\text{-}2$ per decade; Challenging for sub-Edd. cases.

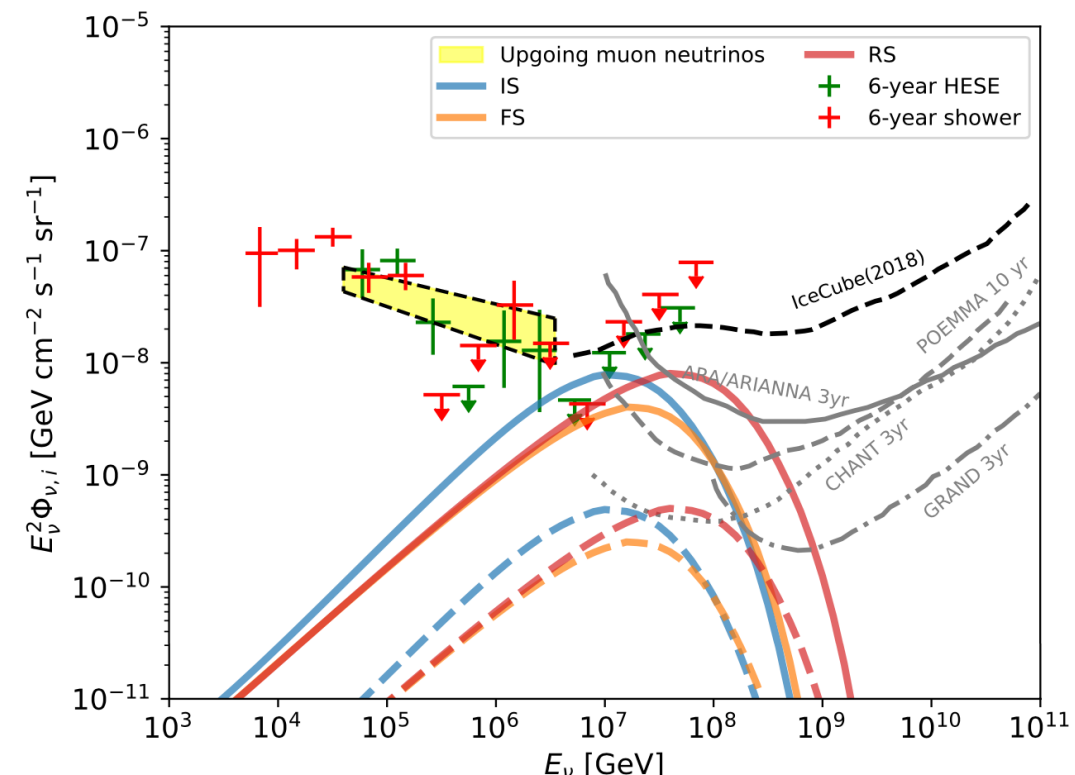
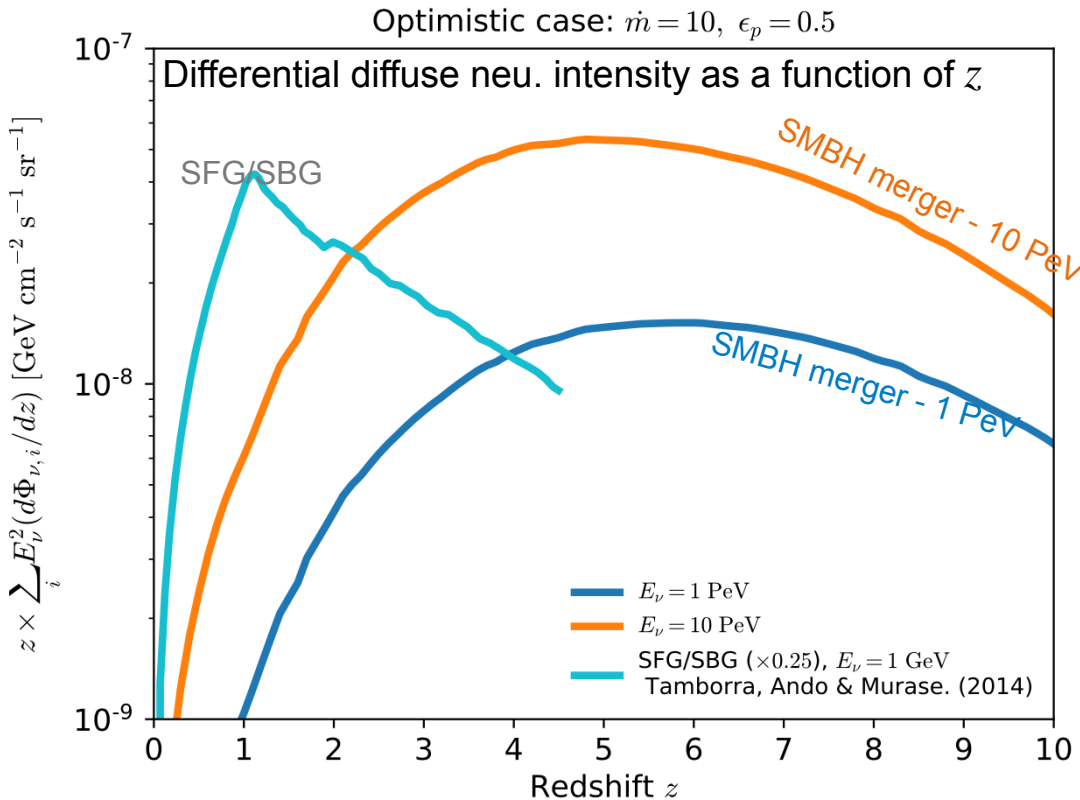
Neutrino detection rate $\dot{N}_{\nu,i}$ for SMBH mergers within the LISA detection range $z \lesssim 6$ [yr^{-1}]

Scenario	Optimistic parameters			Conservative parameters				
	$\dot{m} = 10$, $L_{k,j} \simeq 3.4 \times 10^{46} \text{ erg s}^{-1}$, $\epsilon_p = 0.5$, $h = 0.3$	$\dot{m} = 0.1$, $L_{k,j} \simeq 3.4 \times 10^{44} \text{ erg s}^{-1}$, $\epsilon_p = 0.5$, $h = 0.01$	IC (up+hor)	IC (down)	IC-Gen2 (up+hor)	IC (up+hor)	IC (down)	IC-Gen2 (up+hor)
IS	0.019	0.014	0.13			8.2×10^{-4}	4.3×10^{-4}	3.7×10^{-3}
FS	4.6×10^{-3}	2.8×10^{-3}	0.028			3.5×10^{-5}	2.9×10^{-5}	2.1×10^{-4}
RS	0.011	8.4×10^{-3}	0.044			9.6×10^{-5}	7.2×10^{-5}	4.1×10^{-4}

Yuan et al. 2020

Expected diffuse neutrino flux

- High-redshift SMBH mergers contribute a significant portion comparing to starburst/star-forming galaxies
- Optimistic cases can explain a significant portion of diffuse ν in the **1-100 PeV energy range**. (10% IC diff. neutrinos for sub-Eddington cases)
- Can be tested by next-gen ν detectors, e.g., GRAND, CHANT, ARA/ARIANNA, POEMMA
- Caveat: all mergers are assumed to be identical (increase SMBH mass \rightarrow powerful emission + lower rate), uncertainty with in a factor of 10.

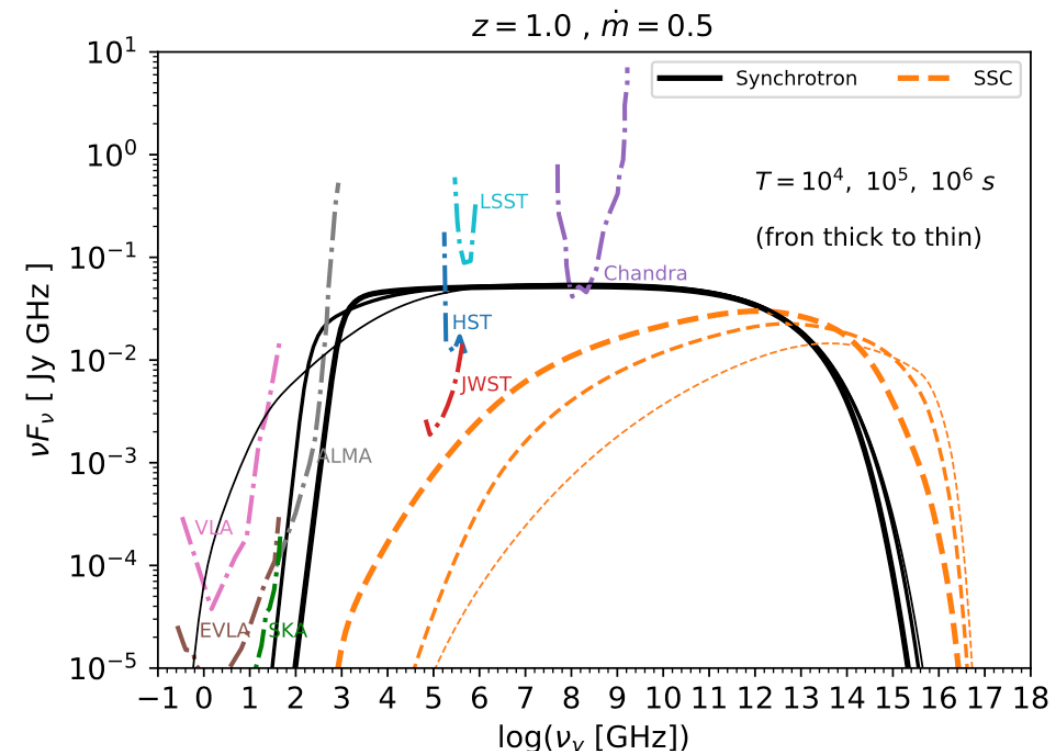
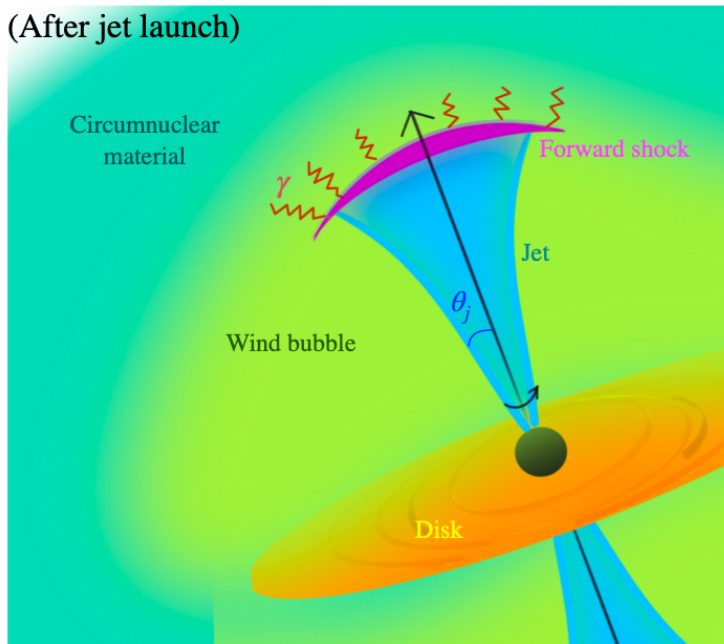
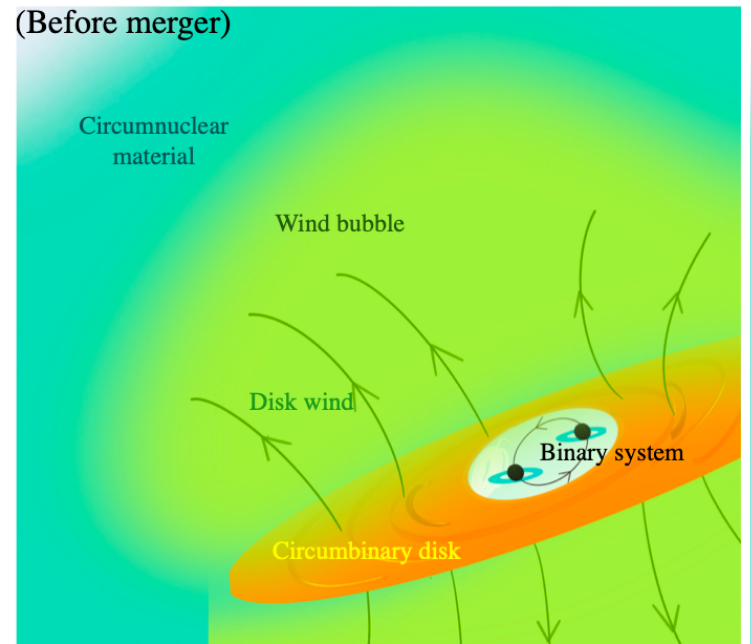


Electromagnetic counterparts: forward shock model

- We consider a sub-Eddington accretor $\dot{M}_{\text{BH}}/\dot{M}_{\text{Eddington}} = 0.5$
- Inside the pre-merger wind bubble (disk-driven winds), the jet is mildly relativistic
 $\Gamma_h \sim \tilde{L}^{1/4}/\sqrt{2} \simeq 2.0$
- Electron injection parameters:
 $dN_e/d\gamma_e \propto \gamma_e^{-2} \exp(-\gamma_e/\gamma_{e,\text{max}})$, $\epsilon_e = 0.01$, $\gamma_{e,\text{min}} = \epsilon_e \zeta_e (\Gamma_h - 1) m_p/m_e$, $\zeta_e = 0.3 - 0.4$
- $\gamma_{e,\text{max}}$ is determined by equating accelerating and cooling

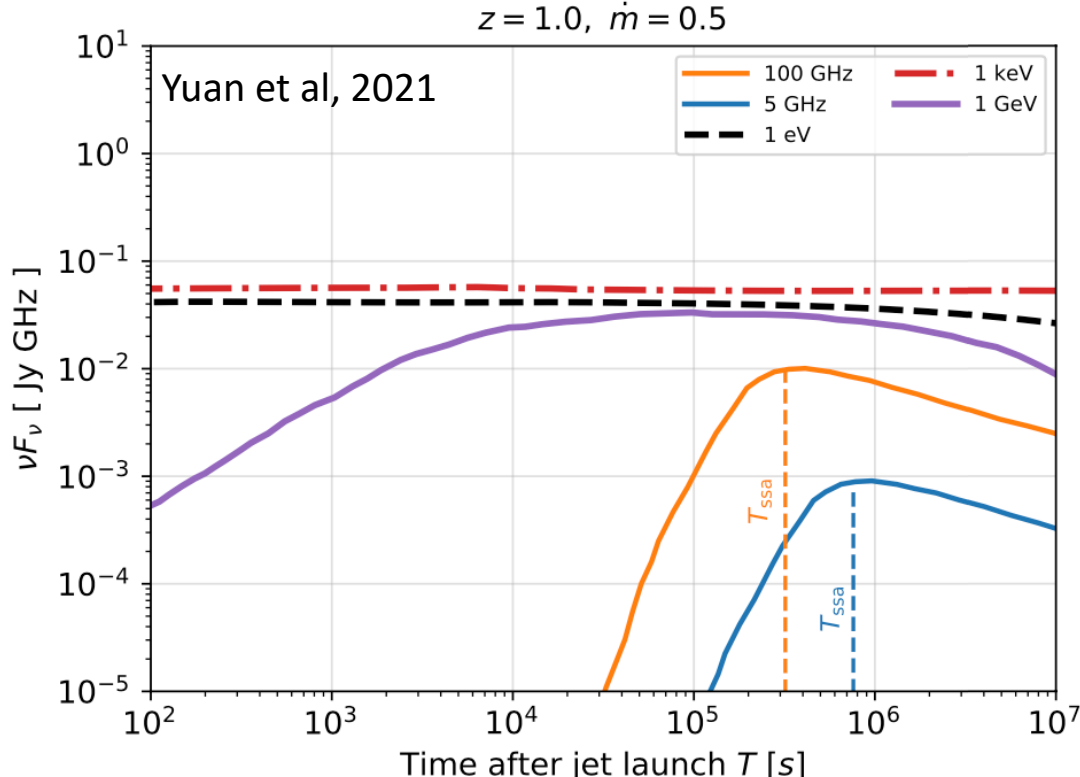
Early radio emission is suppressed by synchrotron self-absorption (SSA)

Non-thermal EM (syn.+SSC) signals are detectable up to the detection horizon of LISA, $(1-10)f_b$ per year



Detection perspectives

- Optical to X-ray fluxes roughly maintain constant while constantly powered jet propagating in the wind bubble.
- After escaping the wind bubble and entering the galactic center ($T_{\text{dur}} \sim 1 \text{ yr}$), the EM signature will look like AGNs
- Early radio emission is suppressed by synchrotron self-absorption (SSA)

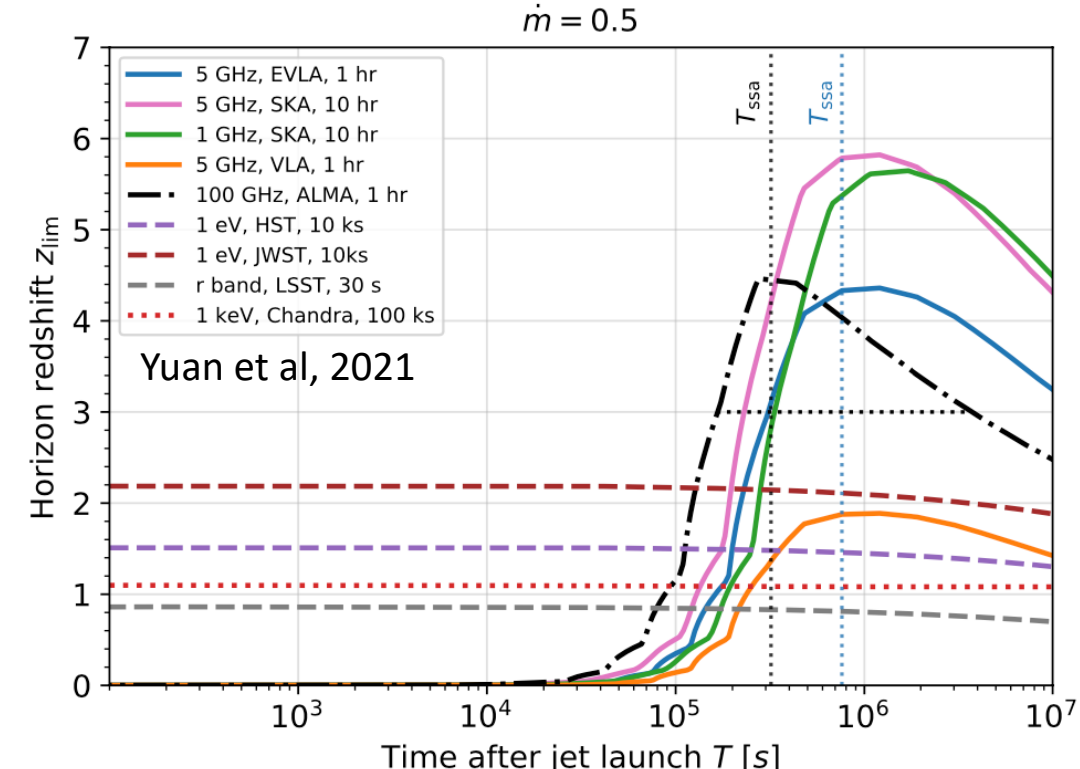


Non-thermal EM (syn.+SSC) signals are detectable up to the detection horizon of LISA, $z \sim 4 - 6$, $(1-10)f_b$ per year

Initial observation with large FOV telescopes (SKA, LSST) can guide narrow FOV detectors.

Multiwavelength
detection horizons

$$d_{\lim}(\nu_\gamma, T) = d_L \left(\frac{\frac{1}{\Delta T_{\exp}} \int_T^{T+\Delta T_{\exp}} F_\nu(\nu_\gamma, t, z) dt}{F_{\lim}(\nu_\gamma, \Delta T_{\exp})} \right)^{1/2},$$



Summary and outlook

- Using the optimistic parameters (super-Eddington accretion rate), IceCube-Gen2 can detect neutrino emission from the LISA-detected SMBH mergers within a decade.
- EM counterpart can be detected up to the horizon of GW detectors, $z = 2\text{-}6$, using VLA, ALMA, SKA, HST, JWST, Chandra, etc...
- These models can be tested by the next-generation gamma-ray/neutrino/GW telescopes. Future multimessenger discoveries would shed more light on the extreme astrophysical objects.
- The SMBH post-merger jets are similar to jetted TDEs. It's exciting to apply jet-wind-cocoon model to jetted TDEs.
- Stay tuned!

In addition to TDEs and SMBH mergers,

1. Diffuse neutrinos and secondary radio/X-ray emission from galaxy mergers

- *Yuan, Meszaros, Murase, Jeong (2018) ApJ*
- *Yuan, Meszaros, Murase (2019) ApJ*

2. VHE gamma-rays from gamma-ray bursts

- *GRB160821B: Zhang, Murase, Yuan, Kimura, Meszaros (2021) ApJL*
- *GRB221009A: Zhang, Murase, Ioka, Song, Yuan, Meszaros (2023) ApJL*

3. Short GRBs embedded in AGN disks

- *Yuan, Murase, Guetta, Bartos, Meszaros (2022) ApJ*

4. Complementarity of Stacking and Multiplet Constraints on the Blazar Contribution to Diffuse Neutrino Flux

- *Yuan, Murase, Meszaros (2020) ApJ*

In addition to TDEs and SMBH mergers,

1. Diffuse neutrinos and secondary radio/X-ray emission from galaxy mergers

- *Yuan, Meszaros, Murase, Jeong (2018) ApJ*
- *Yuan, Meszaros, Murase (2019) ApJ*

2. VHE gamma-rays from gamma-ray bursts

- *GRB160821B: Zhang, Murase, Yuan, Kimura, Meszaros (2021) ApJL*
- *GRB221009A: Zhang, Murase, Ioka, Song, Yuan, Meszaros (2023) ApJL*

3. Short GRBs embedded in AGN disks

- *Yuan, Murase, Guetta, Bartos, Meszaros (2022) ApJ*

4. Complementarity of Stacking and Multiplet Constraints on the Blazar Contribution to Diffuse Neutrino Flux

- *Yuan, Murase, Meszaros (2020) ApJ*

Thanks

Email: chengchao.yuan@desy.de